Magnetic measurement activities at CERN

Part I: projects, infrastructure and collaborations
Part II: instrumentation and techniques

Marco Buzio on behalf of the Test & Measurement Section, Magnet, Superconductors and Cryostat Group

Paul Scherrer Institute, Villigen, 23.05.2023

Test and Measurement Team

- SM18 (superconducting test station) and magnetic measurement teams merged in 2020
- Now 45 strong (20 technical/scientific staff, 17 students, 8 associates and industrial support)
- Slowed-down but not stopped by Covid !

Acknowledgement

Current team members:

Agniezka Chmielinska, Anna Lauria, Carlo Petrone, David Giloteaux, Deepak Paudel, Dimitrios Dardanis, Filip Kosowski, Franco Julio Mangiarotti, Gaelle Ninet, Gerard Willering, Gyu Deferne, Jens Kaeske, Jerome Feuvrier, Lucio Fiscarelli, Luisa Fleig, Mariano Pentella, Matthias Bonora, Melvin Liebsch, Olaf Dunkel, Olivier Ditsch, Pasquale Arpaia, Patrick Viret, Piotr Rogacki, Regis Chritin, Ricardo Beltron, Stephan Russenschuck, Stian Juberg, Unai Martinez, Valentino Scalera, Vera Korchevnyuk, Ville Mattson, Vincenzo di Capua

Accelerator Projects

HL-LHC, super- and normal-conducting magnet projects

High-Luminosity LHC upgrade – Schedule

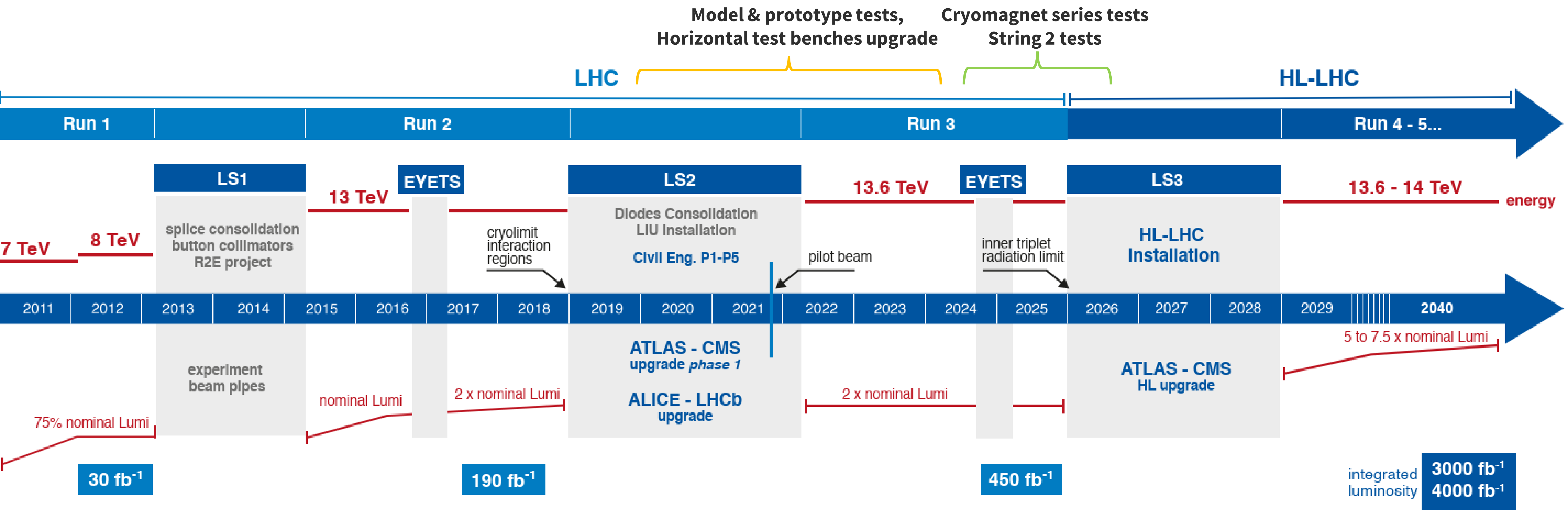

Highest-priority CERN project:

- replace rad-damaged IR quads
- 10 × luminosity → +25% discovery range

High-Luminosity LHC upgrade – Magnet zoo

- ~50 cryomagnets to be measured for LS3
  - 12×∅150 mm, 7.15 m long, 140 T/m MQXF quads
  - 7×∅150 mm, 10-magnet Corrector Packages
  - 7×∅150 mm, 5.6 T MBXF D1 dipoles
  - 7×∅94 mm double-aperture 4.5 T MBRD D2 dipoles
- **First operational accelerator-quality Nb_3Sn** magnets ever
- Magnetic measurement challenges:
  - Up to **∅109 mm anticryostat bores** and 10 m long rotating coil systems
  - very high measurement **accuracy** required
  - 4× warm rotating coil systems to be **maintained abroad** on the manufacturer’s premises
  - **longitudinal alignment** of IR triplets

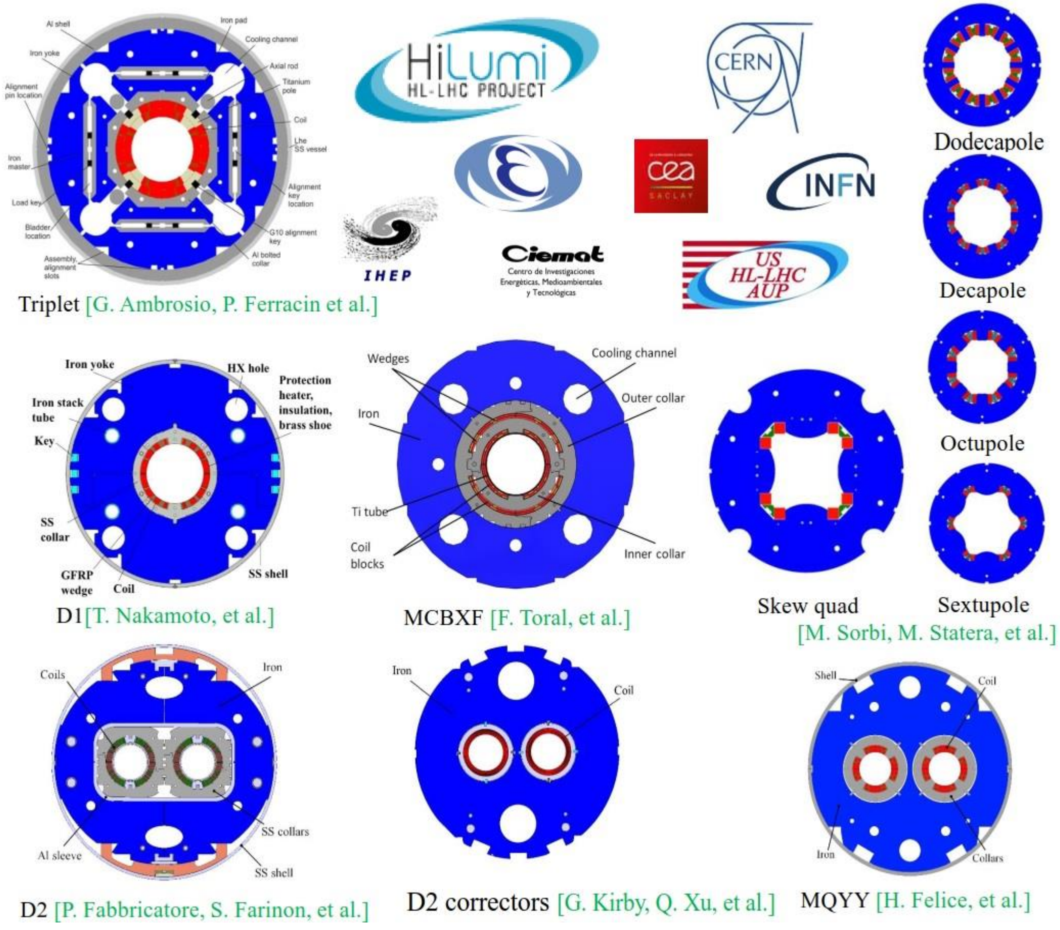

International Superconducting Magnet Projects

High Field Magnets

- 2026 goal: robust Nb_3Sn up to 12T; investigate 16 T potential
- Updated governance, spending profile, manpower
- Recently tested: enhanced Nb3Sn racetrack model coil eRMS (16.5 T peak field @ 13.8 kA, 1.9 K)

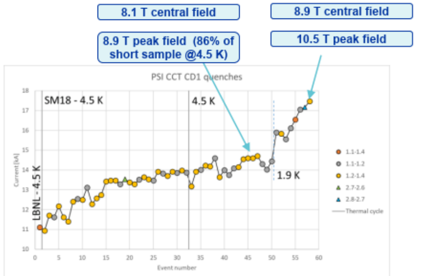

Support to collaborations, *e.g.*, testing at SM18 of PSI CCT Nb_3Sn dipole magnet model

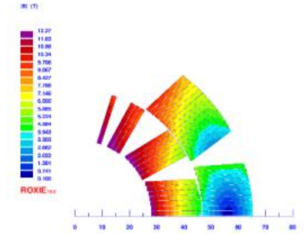

Conceptual design of 12 T robust dipole magnet X-section (based on MQXF cable)

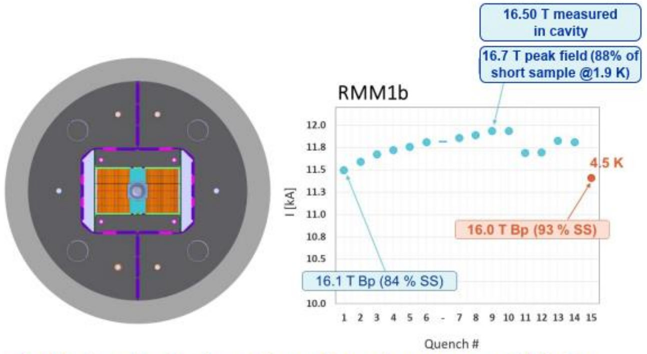

Exploring the limits of in-coil performance of Nb_3Sn

EuCARD[2]

- Networking, transnational access and joint research activities to develop EU accelerator infrastructure
- Recently tested: 5 T Feather M2 dipole with 10 kA ReBCO cable
- Fixed-coil magnetic measurements in a vertical cryostat (not adapted to rotating coils), cross-calibration of coils/Hall probes

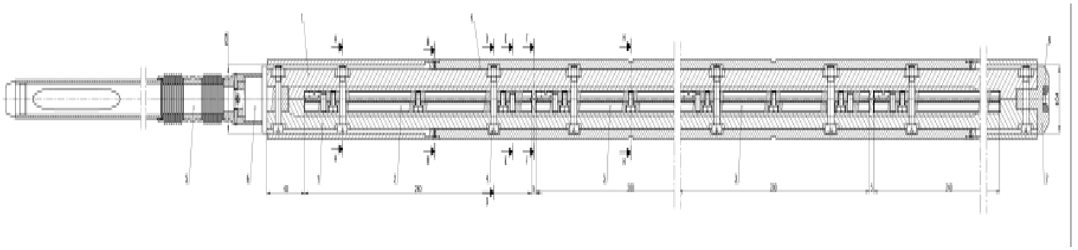

3 × 5 × 200 mm long radial coils

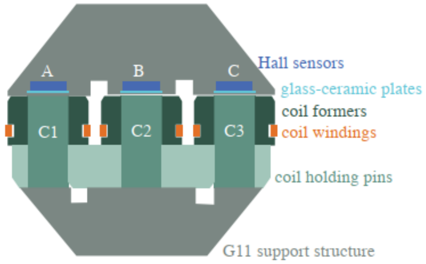

3 × AREPOC LHP-NP Hall probes

FCC - Future Circular Collider

- Focus shifting onto FCC-ee (365 GeV, 100 km tunnel with 57 mT dipoles)
- A few magnets and device prototypes tested so far

SuShi (passive MgB_2 shield for 3T FCC-hh septa)

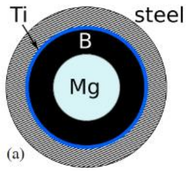

8.3 mm MgB2 thickness
after reactive Mg infiltration

10 × 8 Arepoc HHP-NP (200 mV/T @ 20 mA)
cross-calibrated at RT (relative measurement)

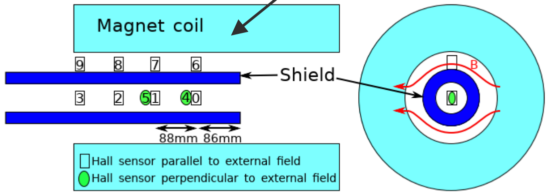

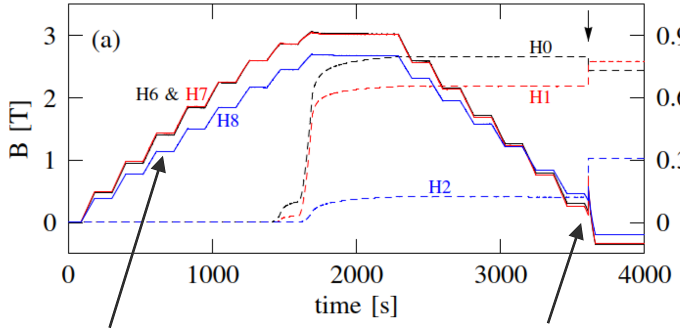

gradual penetration from end

flux jumps at lower field on ramp-down

Credit: C. Petrone

FCC-ee magnets

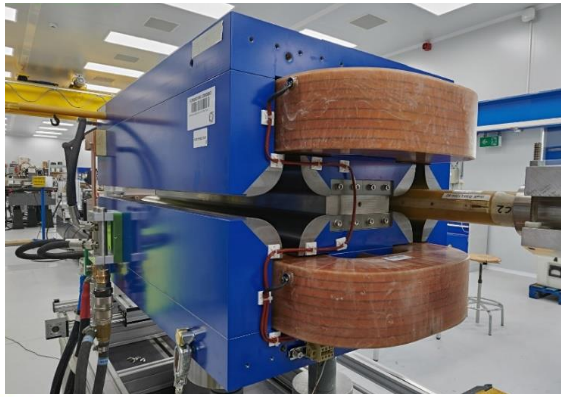

Booster Ring

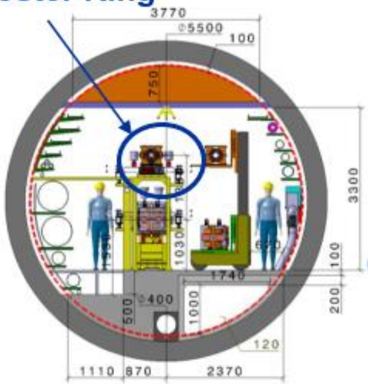

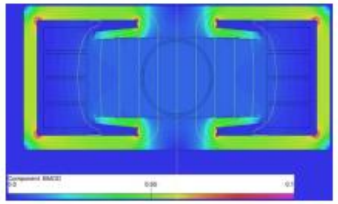

Conceptual design of FCC-ee booster dipole magnet
7 mT (20 GeV) – 63 mT (182.5 GeV)

Refurbishment/upgrade of resistive magnets

- Ageing stock of 5000+ beam line normal-conducting magnets (EOL bathtub curve)
- Common failures: water leaks, insulation integrity → **consolidation and preventive maintenance**
- Occasion for power consumption optimization: DC → pulsed excitation

SPS fixed-target East Area
58 magnets in 2021

new PS extraction bumper with pole face loops
for passive sextupole compensation

LIU – 120 new/refurbished magnets
tested in 2016-2020

SPS fixed-target North Area
(planning under discussion)

Infrastructure

SM18, B. 311, B. 867

SM18 – Magnetic measurement instrumentation

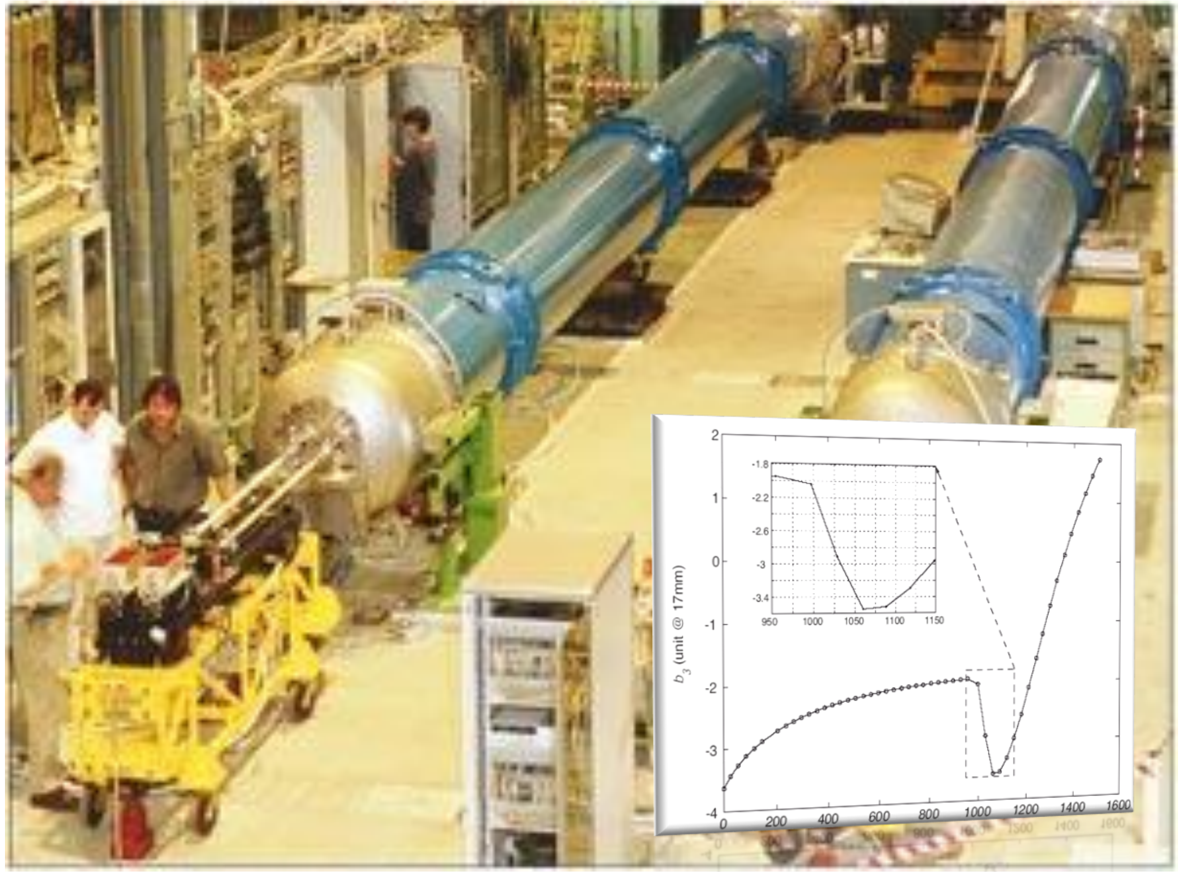

Credit: S. Sanfilippo

(2003) Twin Rotating Units (3 RPM)

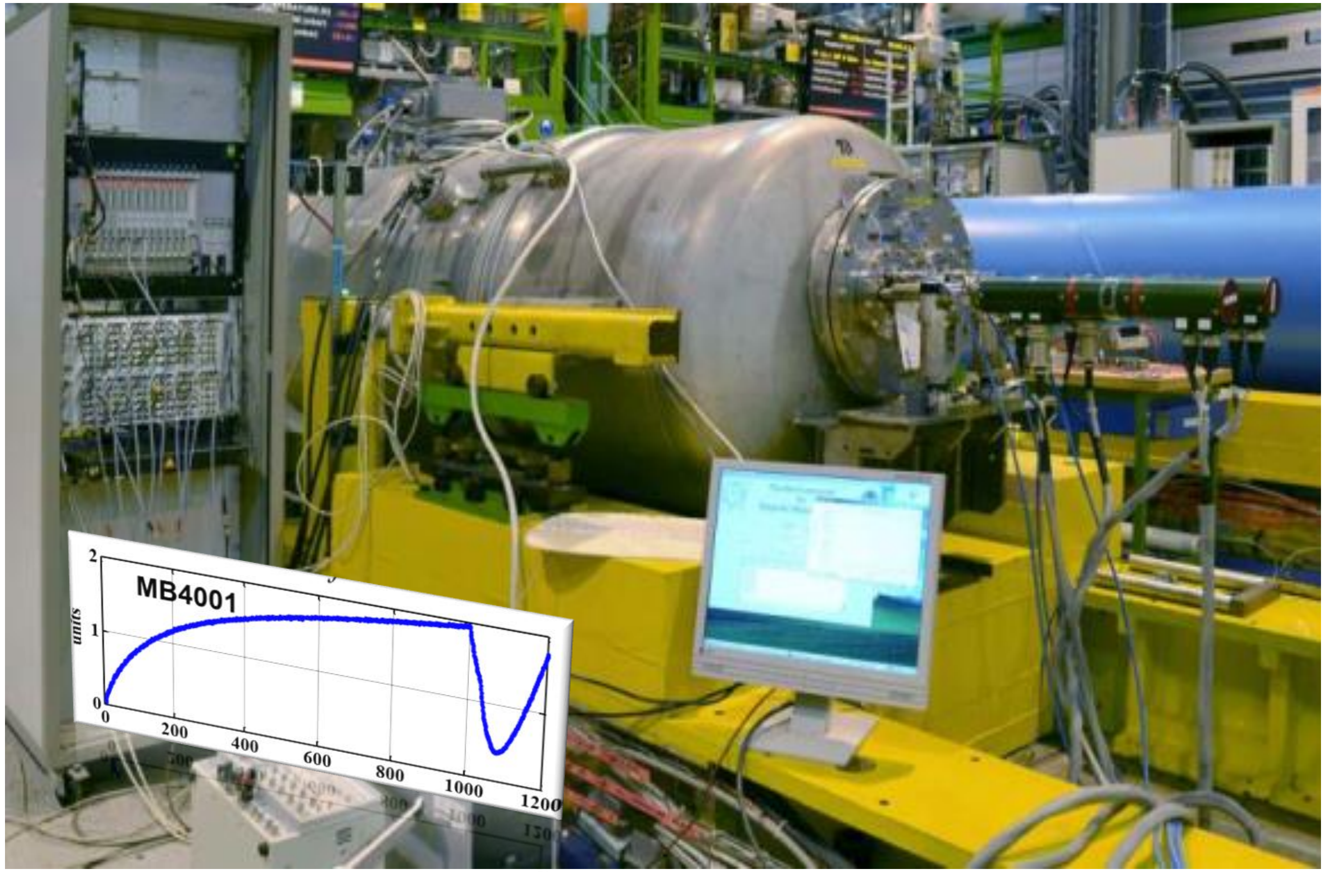

Credit: L. Fiscarelli

(2016) Mobile Rotation Unit (300 RPM)

SM18 Superconducting Test Facility Upgrade

- 4/10 horizontal benches upgraded for HL-LHC cryomagnet, 1/10 for SC Link, 1/10 for coil shaft storage
- Preparations for String 2 under way (25 → 60 g/s Lhe liquefaction, 14 g/s pumping @ 12 mbar)
- Power circuits upgrade: 2×20 kA, 10V converters, 4×2kA auxiliary circuits, load and polarity switches
- DAQ and protection: quench heathers, energy extraction switches, UQDS, CLIQ, PLC & fast interlock systems, anticryostat heaters …

SM18 – Shuffling Module for HL-LHC magnet connection

- Extend and “shuffle” cryogenic lines from CFB to HL-LHC magnets
- Add a phase separator to control LHe level and temperature (4.5 K tests)
- Add 400 W heaters to pre-load He control system (increased ramp losses)
- Add instrumentation (Vtaps, cryo p/T/level sensors)
- 4×units for MQXF, D1/2, CP on A2, B2, C2, F1

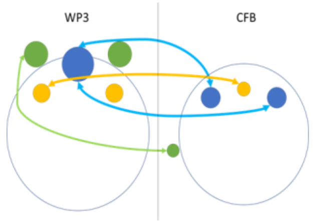

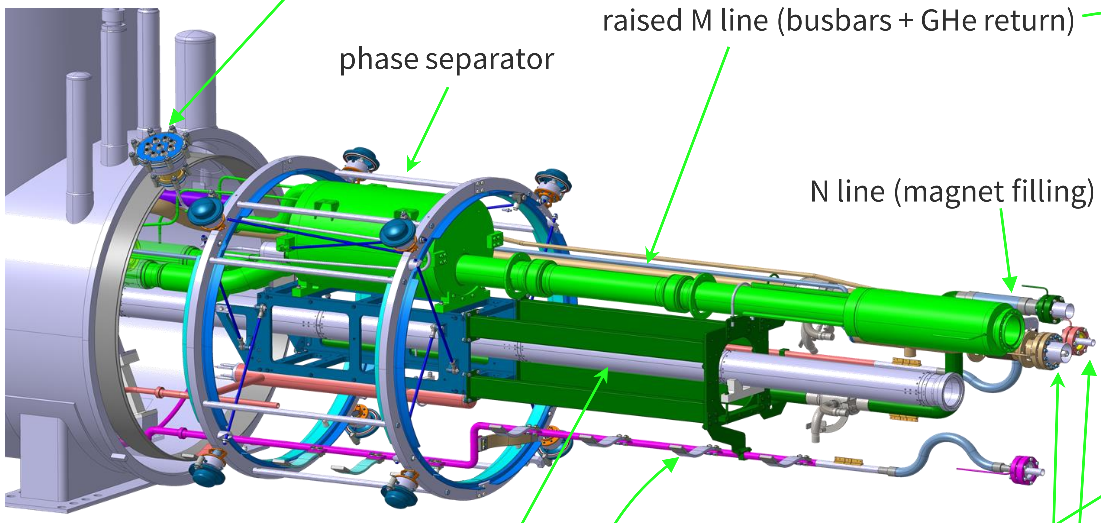

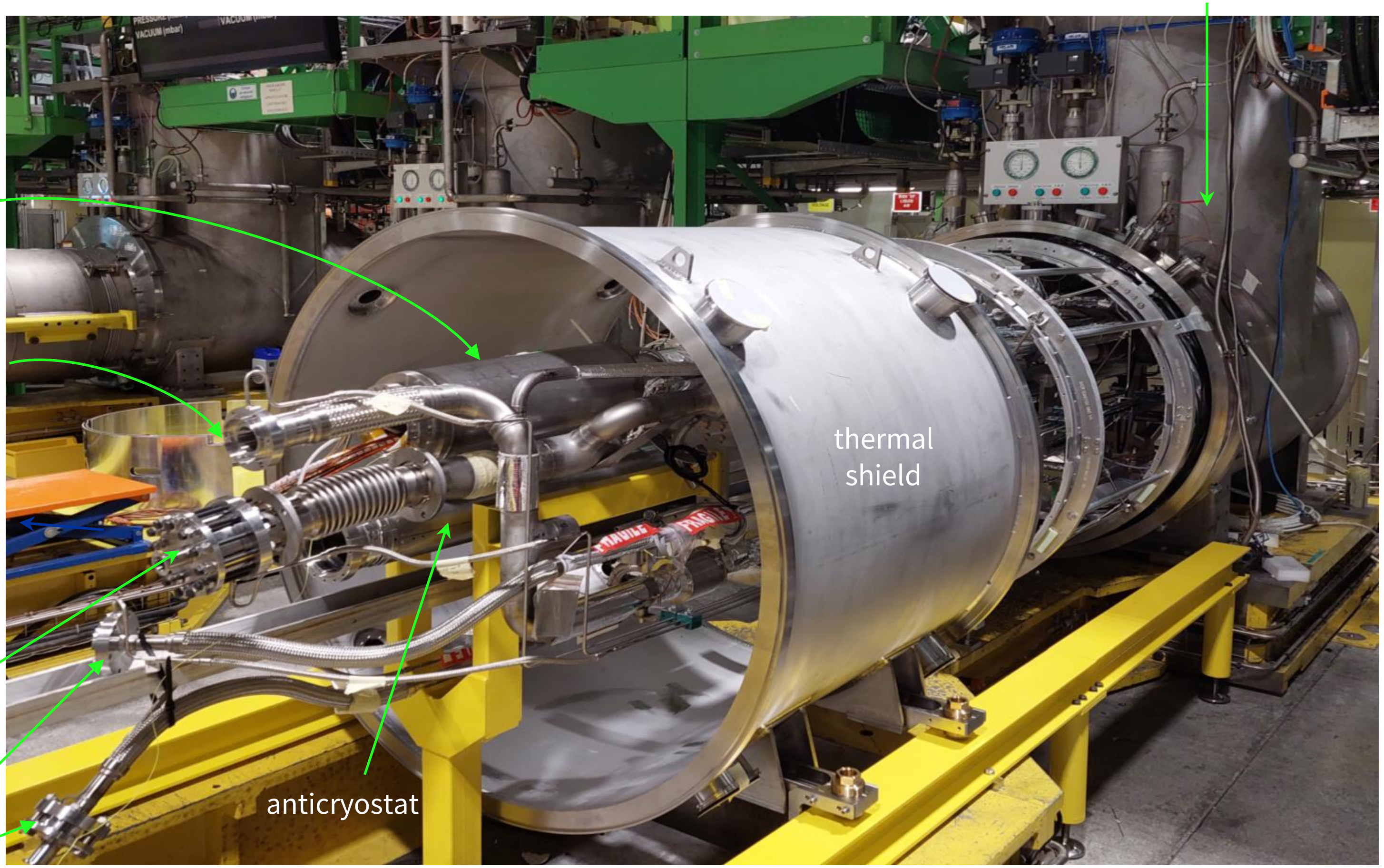

SM18 – F1 bench upgrade for MQXF magnets

4× 2 kA Current Leads

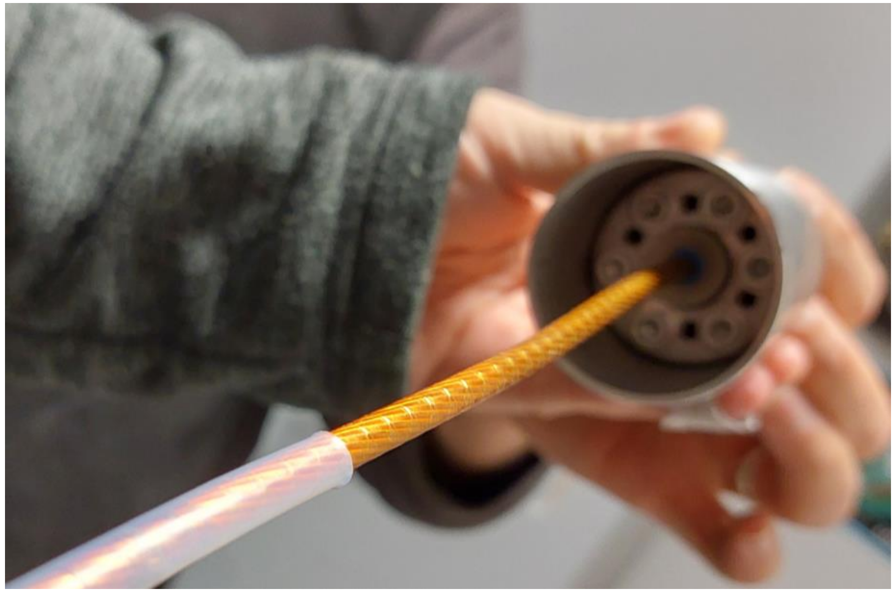

Investigation of HV rigidity of 2 kA current leads plugs

2× 18 kA current leads, to be refurbished with SnAg

Parameter	Value
Resolution (20-bit ADC)	105 nV/LSB .. 48 uV/LSB
ADC speed	Up to 1 MS/s
Analogue bandwidth @ gain	120 kHz @ G=1 90 kHz @ G=9 50 kHz @ G=45 7 kHz @ G=450
Active input voltage range	+/-50 mV (G=450) .. +/-22.5 V (G=1)
Max differential input voltage	1 kV/1 s
Galvanic insulation	2.5 kV/20 min

- Universal Quench Detection System: modular electronics for NbTi, Nb_3Sn, MgB_2 and HTS elements
- Redundant, current-dependent detection based on coil-to-coil and aperture-to-aperture comparison
- Up to 16 ch./crate
- Remote configuration and diagnostics (Ethernet/FESA)

F2 bench upgrade for the SC Link

- 5×130 m (matching sections) + 5×100 m (triplets) SC links to power the new IR from the surface
- 4×18 kA + 12×2kA + 3×7kA MgB_2 conductors @ 5~33 K

SM18 - Vertical Test Stations

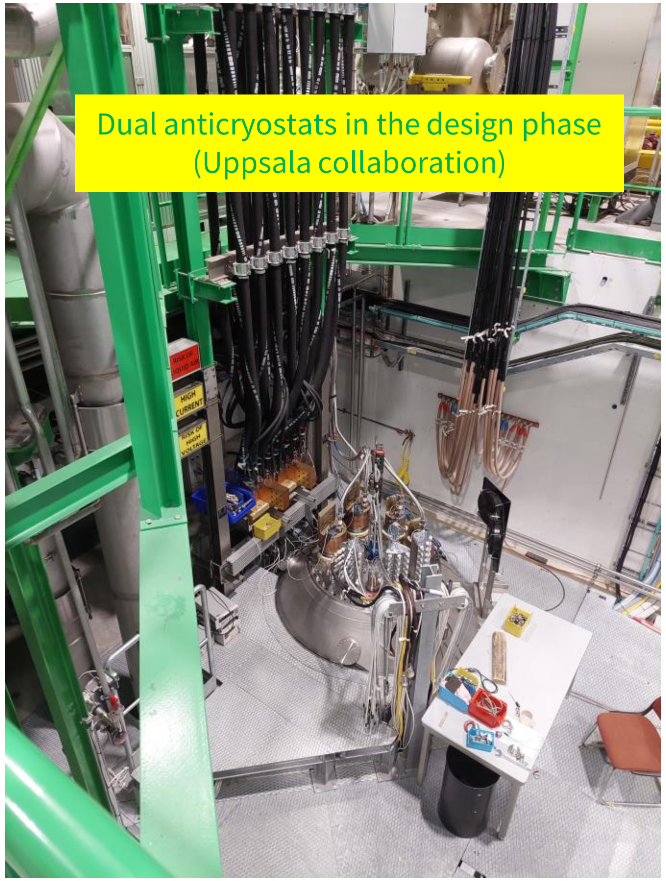

Bench Cluster D
up to ∅600 mm × 5.5 m magnet
1 × 30 kA + 2 × 2kA converters

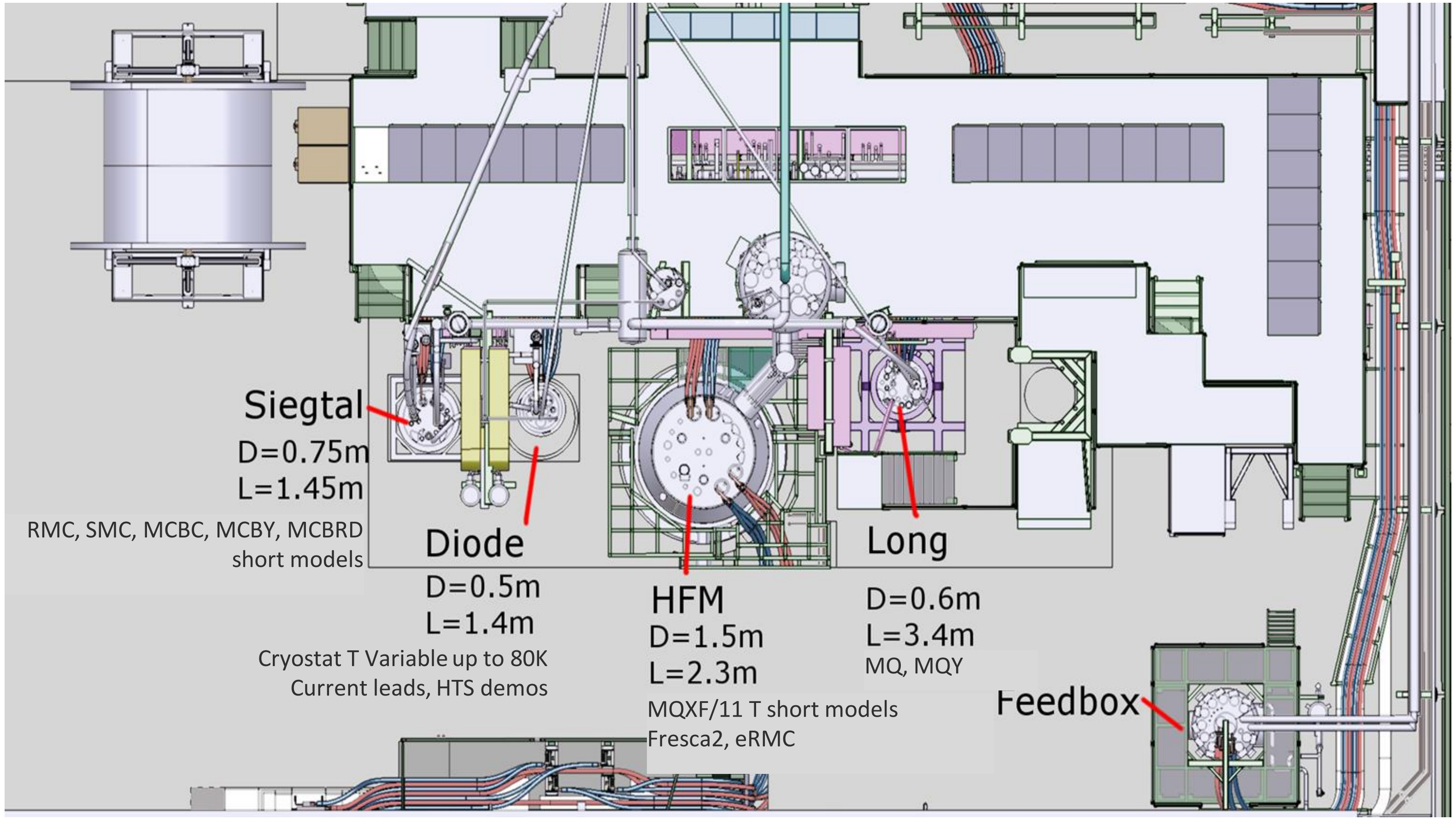

Bench Cluster G (aka "Bloc 4")
consolidation under discussion: safety load switches, new 20 kA energy extraction

B. 311 – Resistive Magnet Test Facility

- Finished in Dec 2017 at the cost of 7.5 MCHF (well on time and within budget)
- 1600 m² on two floors, 17 independent test benches, 2 × water cooling circuits
- 40-ton crane (adequate for all beam-line magnets in the complex)
- Thermal stabilization 21±1.5 °C
- 15+ rotating coil systems ∅8 to 300 mm, 150 mm to 2.5 m length

B. 311 – Powering infrastructure

- Requirement: safe, high-turnover magnet connections (50~100 tests/year); full current cycle programming flexibility
- 8 × converters up to 1 kA/120 V, 750 A DC/120 V, 400 A/450 V, switchable onto 17 benches
- Motorized circuit breakers + blade switches, 750 A DC cables, interlocks, diagnostics

CERN COMET 4P converter

Circuit breaker array

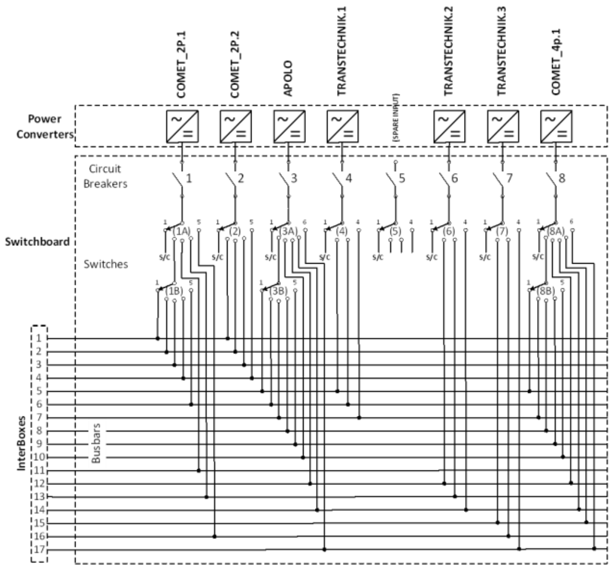

sparse bench/converter connection matrix

Current readout interlock controls

test bench connection box

UNIVERSAL SERIAL BUS

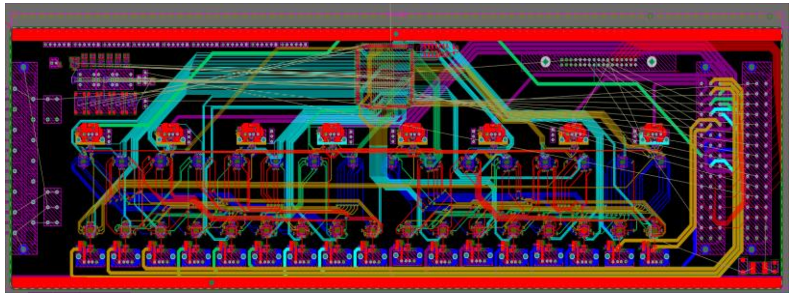

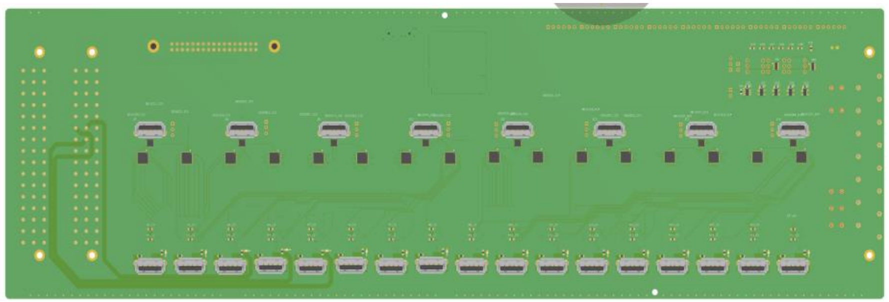

In-house developed **17×8** bidirectional USB matrix switch, freely available on https://ohwr.org

B. 311 – Calibration facility

2 × 2.5 m reference dipoles, 80 mm gap
2.61 Tm @ 316 A, 1.5 T peak field, NMR-mapped
- Int. strength cross-check
- Calibration of coils and other sensors
- Material and component tests

2 × 1.55 m reference quads
∅125 mm bore
13.33 T, 9.5 T/s @ 450 A
L = 1.55 m
- Int. gradient cross-check
- Int. roll angle calibration
- Fiducialization (centering)

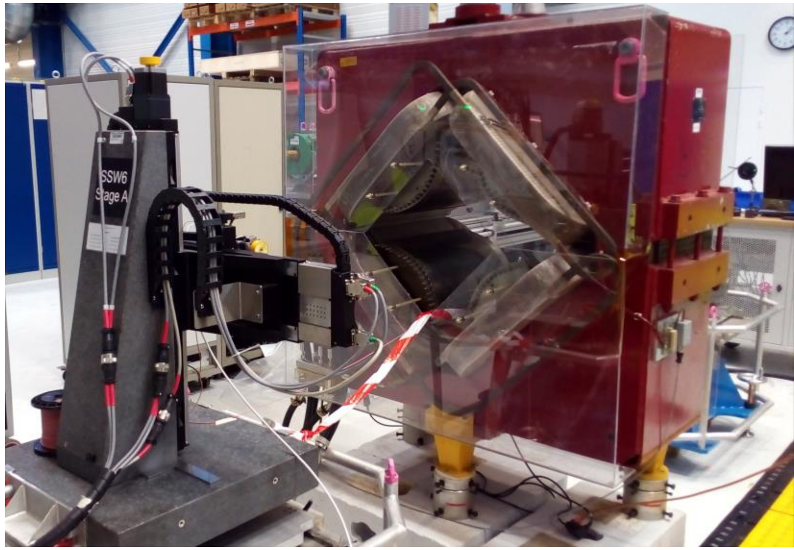

∅350 mm gap reference quad
calibration of large rotating coils

Narrow AC mumetal dipole (long coil width calibration)

B. 311 – T-stabilized test hall

- Separated high-accuracy test hall Class 2 (VDI/VDE 262) with high mechanical/thermal stability (21±0.2 °C)
- Optimized AC airflow for resonant vibrating wire systems

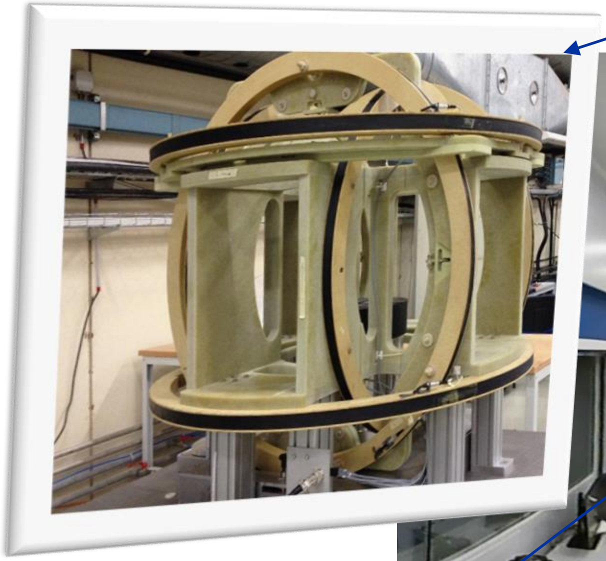

867 – Large magnet test hall (radiocontrolled)

New BOREAL PC (planned):
±6 kA RMS, ±320V

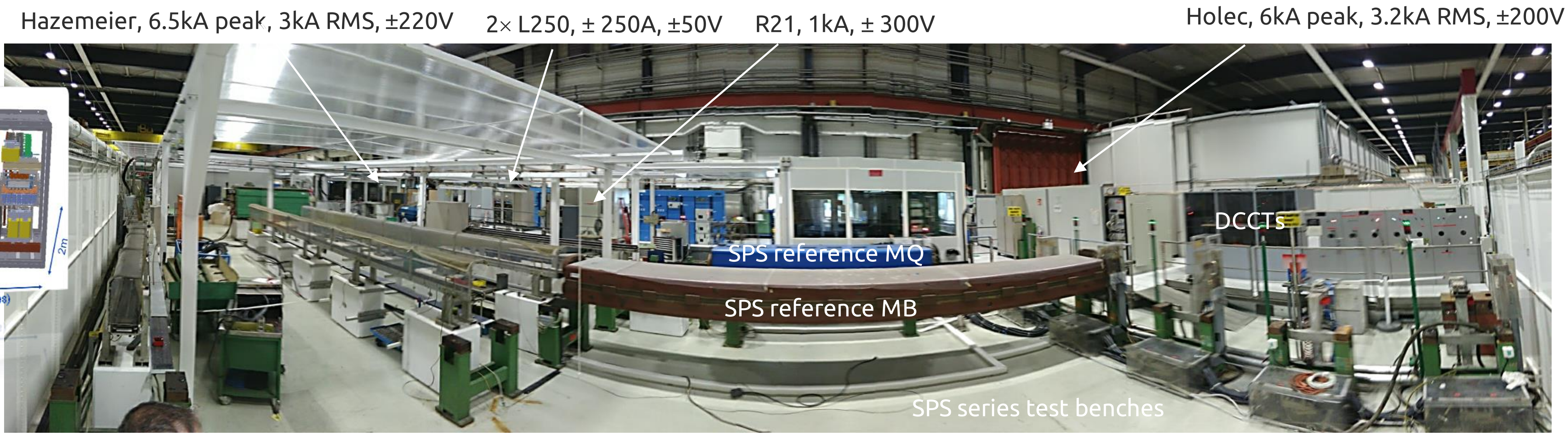

Collaborations

International Collaborations

GSI/FAIR Super-FRS magnet test station in b. 180

- 26 multiplets (170 magnets) + 24 bending dipoles, super-ferric with supercritical He cooling
- very large warm bores: ∅192 (multiplets), 380 × 180 mm (dipoles)
- tests ramping up on 3 reconfigurable benches (b. 181)

DIETI UNIVERSITA' DEGLI STUDI DI NAPOLI FEDERICO II
DIPARTIMENTO DI INGEGNERIA ELETTRICA E DELLE TECNOLOGIE DELL'INFORMAZIONE

IMPALAB INSTRUMENTATION & MEASUREMENT for Particle Accelerator Lab

TECHNISCHE UNIVERSITÄT DARMSTADT

PAUL SCHERRER INSTITUT PSI

POLITECNICO MILANO 1863

iter
china eu india japan korea russia usa

INFN LNF
Istituto Nazionale di Fisica Nucleare

UPPSALA UNIVERSITET

RWTH AACHEN UNIVERSITY

universität wien

L-Università ta' Malta

Collaboration CERN-PSI

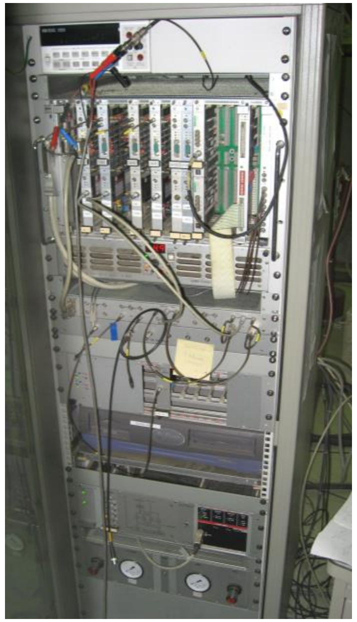

- Formal basis: **Framework Collaboration Agreement K1635/DG**
- (2008) QIMM Mole ∅38mm: Agreements **K1561/AT** (Loan), **K1686/TE** (purchase)
- (2011) Linac 2 bench: purchase Agreement **KR1844/TE**
- (2016) Upgrade of DAQ systems/software by a transferred student (P. La Marca)
- (2017) PCB coil design and calibration
- (2018) **∅8mm sapphire coil shaft** (G. Severino)
- (2021) Measurement of magnetic steel properties

.....

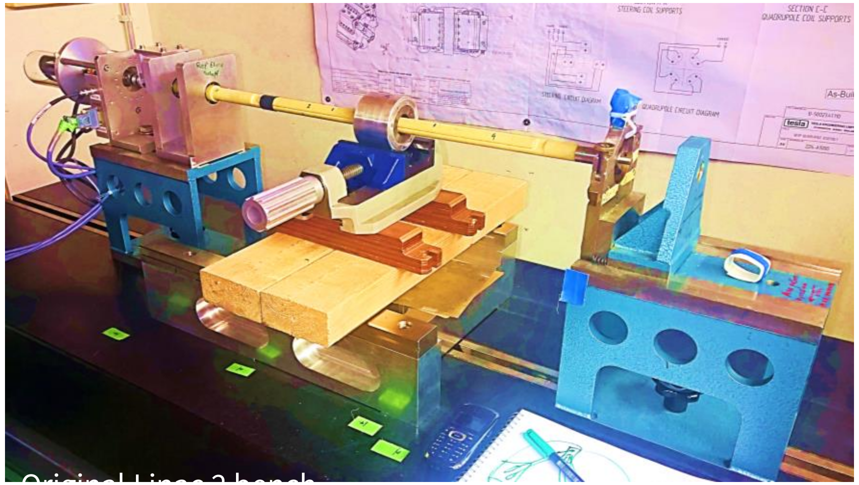

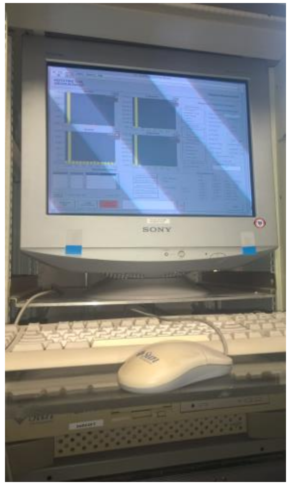

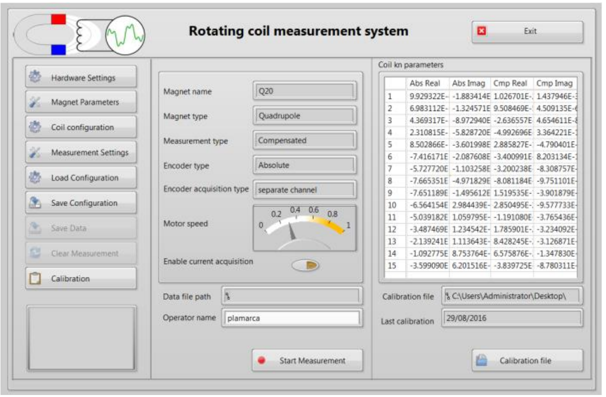

P. La Marca, Rotating coil acquisition system based on NI DAQ, CERN Internship Report, 2016
P. La Marca, Upgrade of rotating coil systems for accelerator magnets, PhD thesis, Politecnico di Milano, 2017

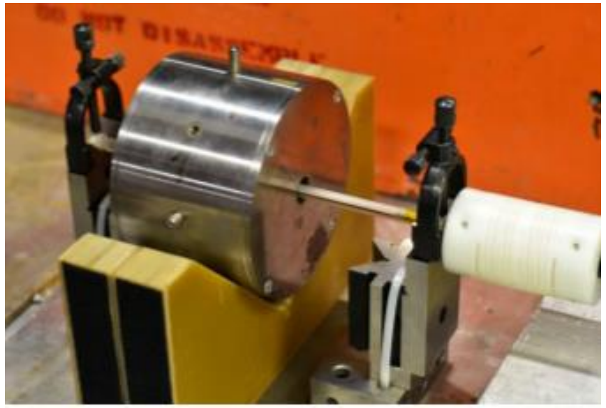

G. Severino, High-precision miniaturized rotating coil transducer for magnetic measurements, Sensors, 2018

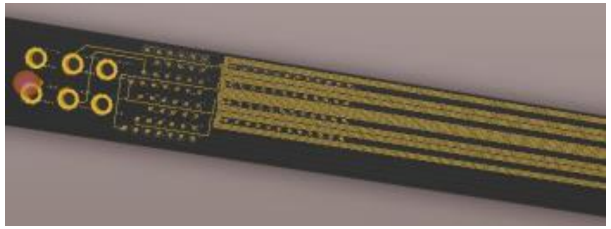

Collaboration CERN-ITER

- (2008) Formal framework: CERN-ITER co-operation agreement **KR1449**
- Subsequent **implementing agreements** on many topics: rad-hard electronics, HTS leads, vacuum leaks, safety interlocks, insulation …
- (2014) magnetic permeability of **co-wound tape** for TF coil quench detection

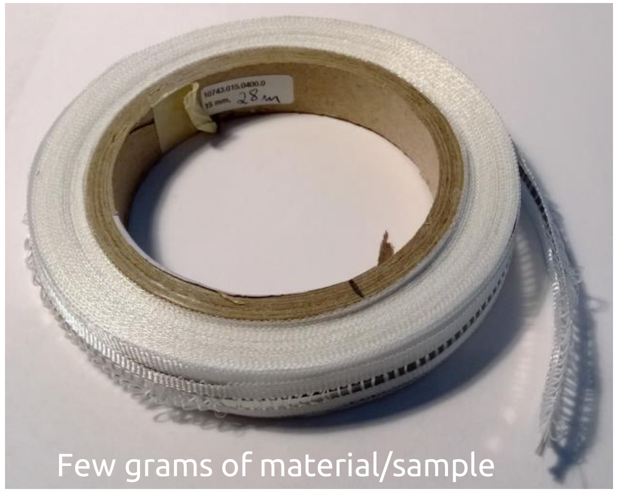

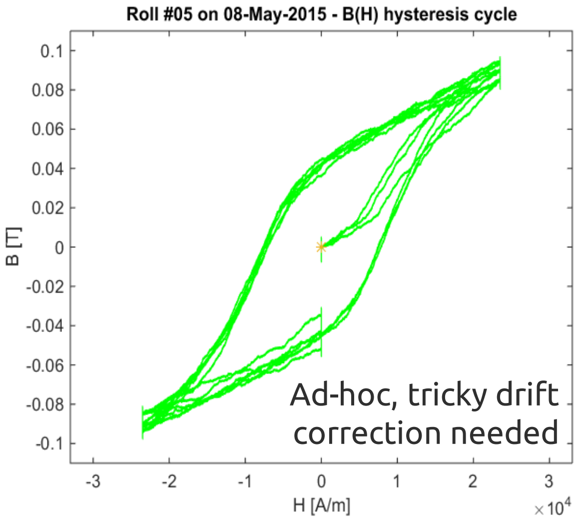

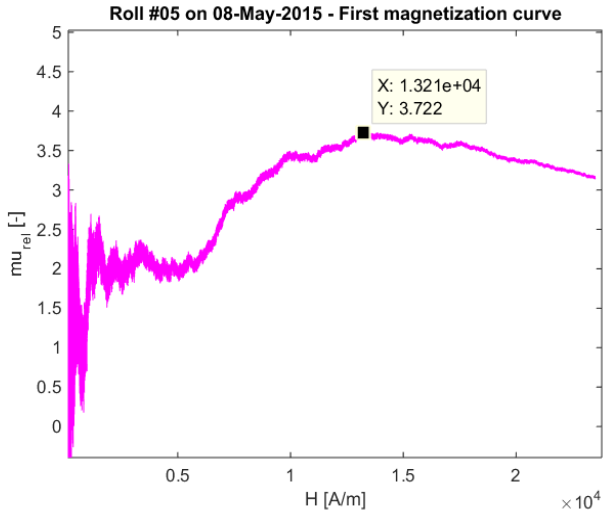

Toroidal ring samples tested in the split-coil permeameter

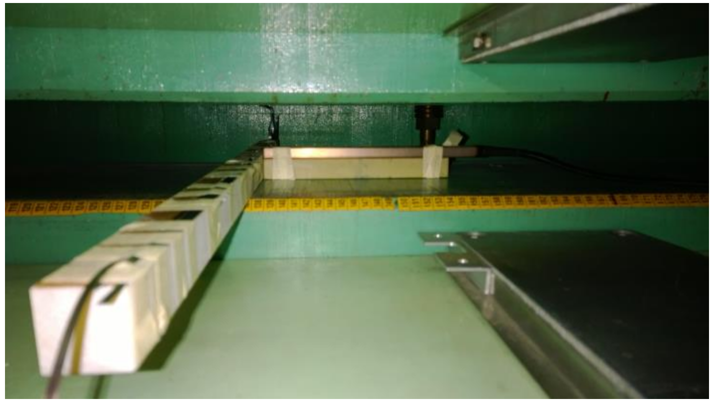

Straight samples tested open-circuit in 1T field

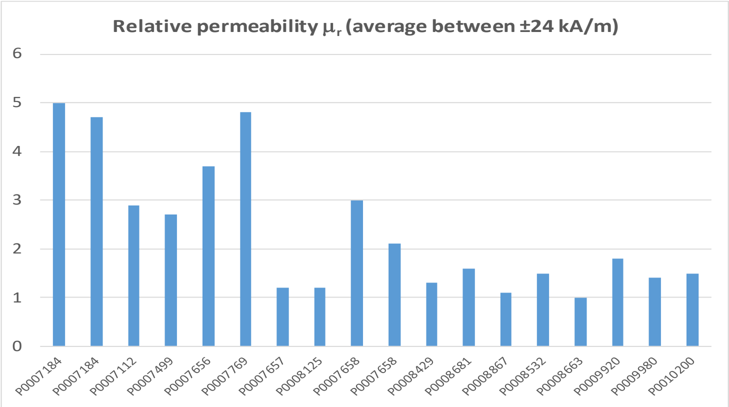

ITER – TF Coil CCL reconstruction (1/5)

- Objective: measure the **equivalent Current Center Line of the TF coils**, to inform final assembly
- Difficult, ill-posed problem requiring an innovative solution
- Indirect but fruitful collaboration between PSI (focus on acquisition setup) and CERN (focus on CCL reconstruction)
- Chosen strategy: AC excitation of the TF coil + inductive measurement of the field pattern all around it

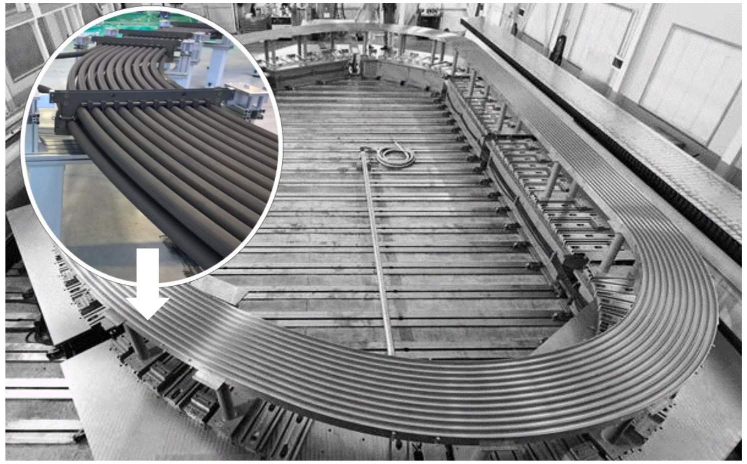

1D example:

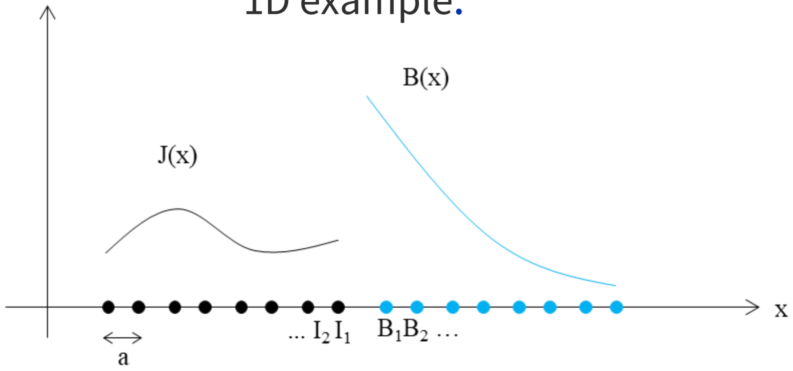

$$B_{yj} = \frac{\mu_0}{2\pi}\sum_k \frac{I_k}{x_j - x_k} = \frac{\mu_0}{2\pi a}\sum_k \frac{I_k}{j+k-1}$$

$$\frac{\mu}{2\pi a} HI = B_y \qquad H = \begin{bmatrix} 1 & \frac{1}{2} & \cdots & \frac{1}{n} \\ \frac{1}{2} & \frac{1}{3} & & \frac{1}{n+1} \\ \vdots & & \ddots & \vdots \\ \frac{1}{n} & \frac{1}{n+1} & \cdots & \frac{1}{2n-1} \end{bmatrix}$$

Hilbert matrix

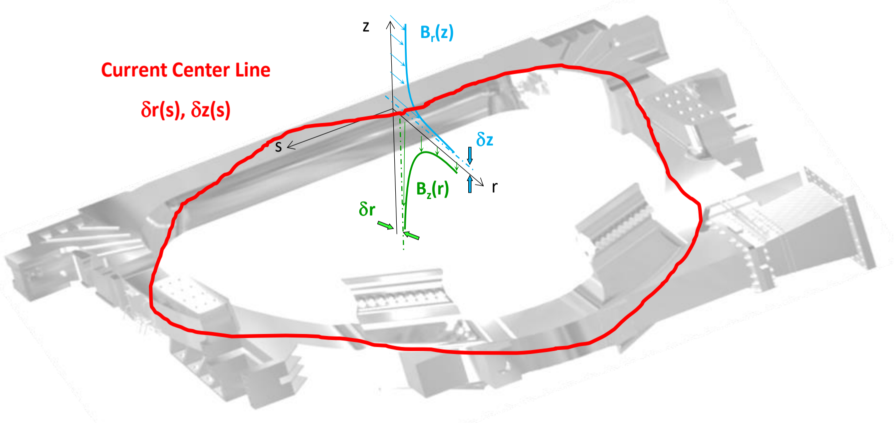

$$\kappa(H) = \|H\|_2 \|H^{-1}\|_2 = \frac{max\ \lambda(H)}{min\ \lambda(H)} \propto \frac{(1+\sqrt{2})^{4n}}{\sqrt{n}} \qquad \frac{\|\Delta I\|_2}{\|I\|_2} \le \kappa(H)\frac{\|\Delta B\|_2}{\|B\|_2}$$

linear problem, but condition number $\kappa \sim 10^3$ already for n=2 !
Regularization needed

WP11 test campaign ASG La Spezia, IT

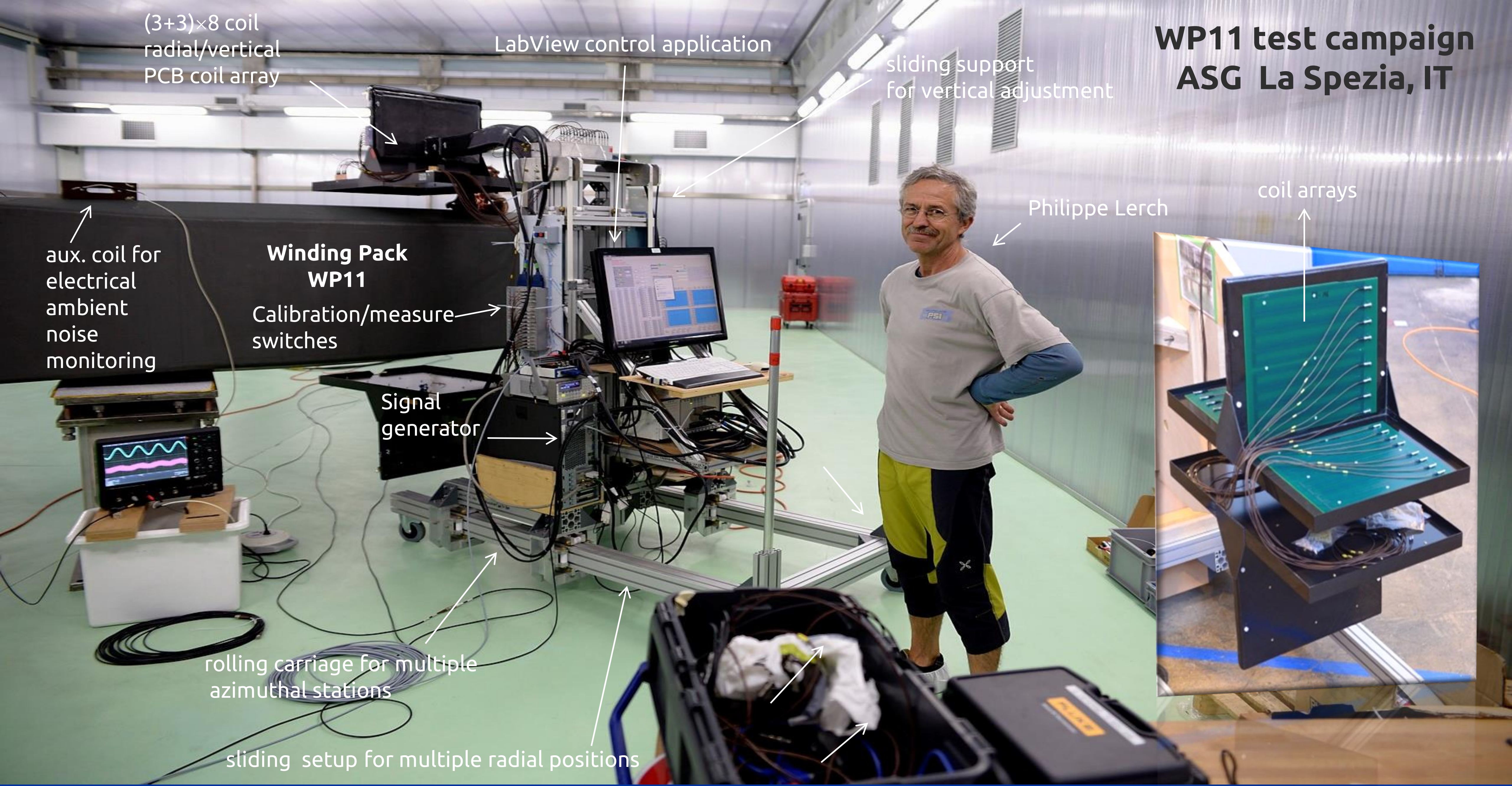

ITER – TF coil CCL reconstruction (3/5)

Regularized reconstruction method: minimize difference between measured and computed field w.r.t. a set of discrete variables **δ** = amplitudes of low-order deformation modes

$$\chi^2(\boldsymbol{\delta}) = \sum_k \frac{\left(B_k^{meas} - B_k(\boldsymbol{\delta})\right)^2}{\sigma_{B_k}^2} = \left(\boldsymbol{W}\Delta\boldsymbol{B}(\boldsymbol{\delta})\right)'\left(\boldsymbol{W}\Delta\boldsymbol{B}(\boldsymbol{\delta})\right) \approx \chi^2(\boldsymbol{\delta}_0) + \nabla\chi^2\Delta\boldsymbol{\delta} + \frac{1}{2}\Delta\boldsymbol{\delta}'\boldsymbol{H}\Delta\boldsymbol{\delta} + \dots$$

$$\boldsymbol{J} = \left[\frac{\partial B_k}{\partial \delta_j}\right]$$

$M\times N$ magnetic field Jacobian matrix

$$\boldsymbol{W} = diag\left[\frac{1}{\sigma_{B_k}}\right]$$

$M\times M$ weight matrix (inverse uncertainty

$$\Delta\boldsymbol{B} = \boldsymbol{B}^{meas} - \boldsymbol{B}(\boldsymbol{\delta})$$

$M\times 1$ measured-computed field difference vector

$$\nabla\chi^2 = -\sum_k \frac{B_k^{meas} - B_k(\boldsymbol{\delta})}{\sigma_{B_k}^2}\frac{\partial B_k}{\partial \delta_j} = \boldsymbol{W}\Delta\boldsymbol{B}\,\boldsymbol{W}\boldsymbol{J}$$

$M\times 1$ gradient vector

$$\boldsymbol{H} = \left[\frac{\partial^2\chi^2}{\partial\delta_i\partial\delta_j}\right] \approx (\boldsymbol{W}\boldsymbol{J})'\boldsymbol{W}\boldsymbol{J}$$

$N\times N$ Hessian matrix (omitting by default second derivative terms)

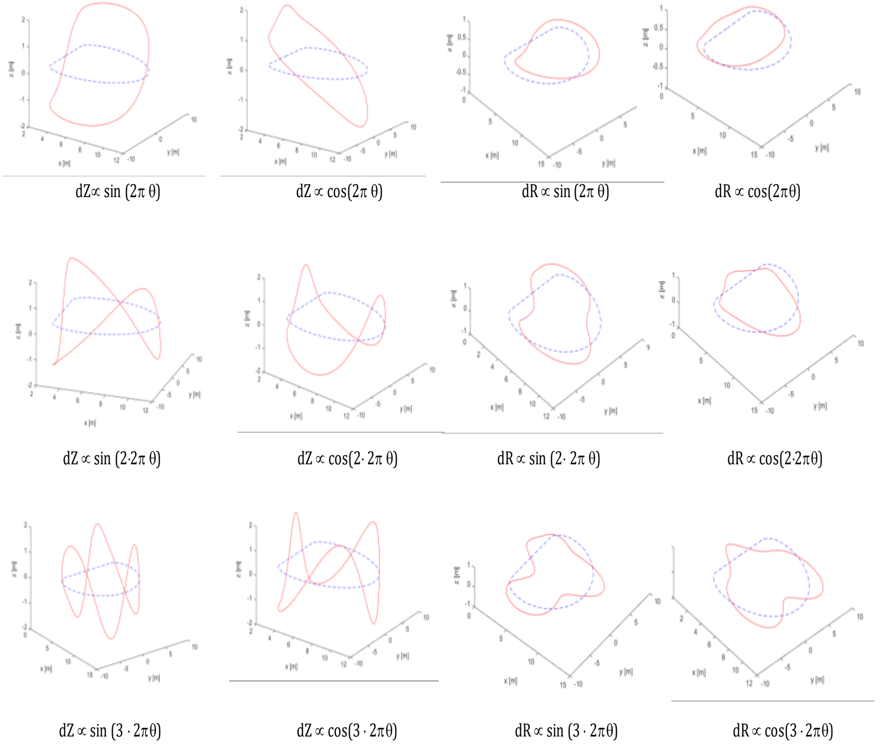

find iteratively the d.o.f. increment Δδ that satisfies:

(linear approximation) $\chi^2(\boldsymbol{\delta}) = 0 \;\Rightarrow\; 0 = -\boldsymbol{W}\Delta\boldsymbol{B}(\boldsymbol{\delta}_0) + \boldsymbol{W}\boldsymbol{J}\,\Delta\boldsymbol{\delta} \;\Rightarrow\; \Delta\boldsymbol{\delta} = (\boldsymbol{W}\boldsymbol{J})^{\dagger}\Delta\boldsymbol{B}(\boldsymbol{\delta}_0)$

(quadratic approximation) $\min\chi^2(\boldsymbol{\delta}) \;\Rightarrow\; 0 = -\boldsymbol{W}\boldsymbol{J}\Delta\boldsymbol{B}(\boldsymbol{\delta}_0) + \boldsymbol{H}\,\Delta\boldsymbol{\delta} \;\Rightarrow\; \Delta\boldsymbol{\delta} = \boldsymbol{H}^{\dagger}\boldsymbol{W}\boldsymbol{J}\Delta\boldsymbol{B}(\boldsymbol{\delta}_0)$

$$(\boldsymbol{W}\boldsymbol{J}\ or\ \boldsymbol{H}) = \boldsymbol{U}\ diag\left[s_j\right]\boldsymbol{V}$$

$$(\boldsymbol{W}\boldsymbol{J}\ or\ \boldsymbol{H})^{\dagger} = \boldsymbol{V}'diag\left[\begin{cases} if\ \frac{s_j}{s_1} > tol, & \frac{1}{s_j} \\ if\ \frac{s_j}{s_1} \le tol, & 0 \end{cases}\right]\boldsymbol{U}'$$

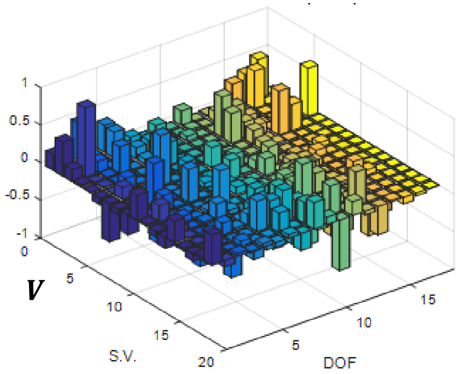

identify linear combinations of d.o.f. that correspond to small singular values and degrade system conditioning

variance of estimated parameters:

$$\sigma_j^2 = diag(\boldsymbol{H}^{-1})$$

correlation terms ignored up to now ⇒ possibile overstimation of error bars

ITER – TF Coil CCL reconstruction (4/4)

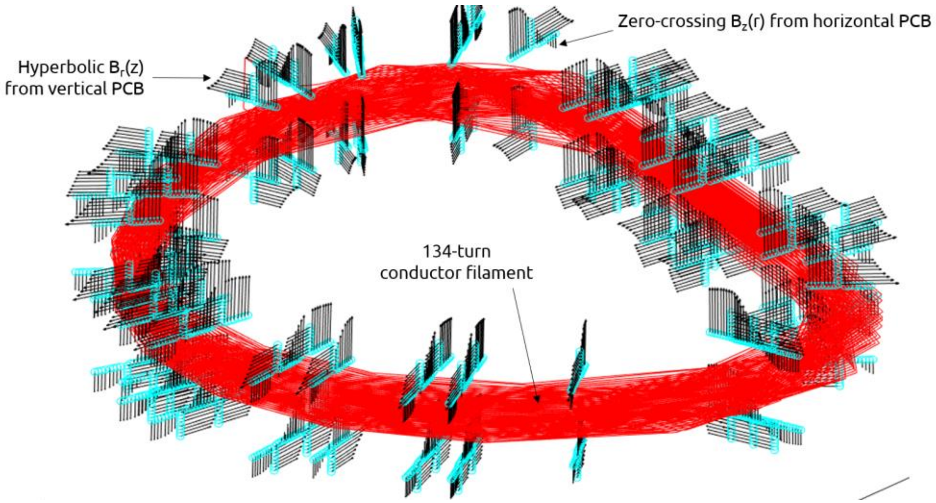

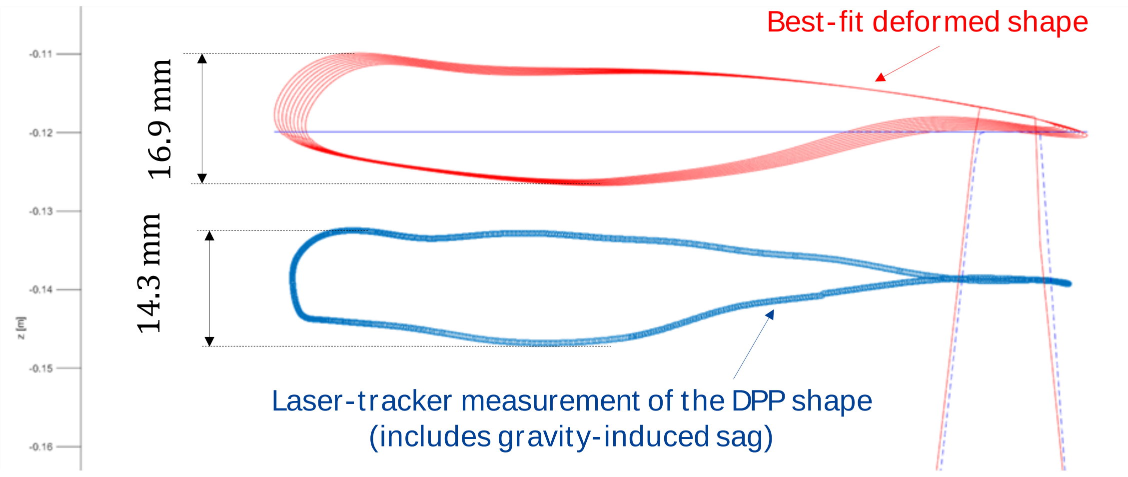

- **7200** data points @ 35~38 A = 48 pick-up c5ils × 50 stations × (0.1, 0.15 and 0.2 Hz)
- Max. measured field: **1640 μT** (radial), 1360 μT (vertical)
- Max. measured gradient: 2.7 μT/mm (radial), **3.4 μT/mm** (vertical)

Dual-pancake prototype reconstruction uncertainty: ±1.2 mm

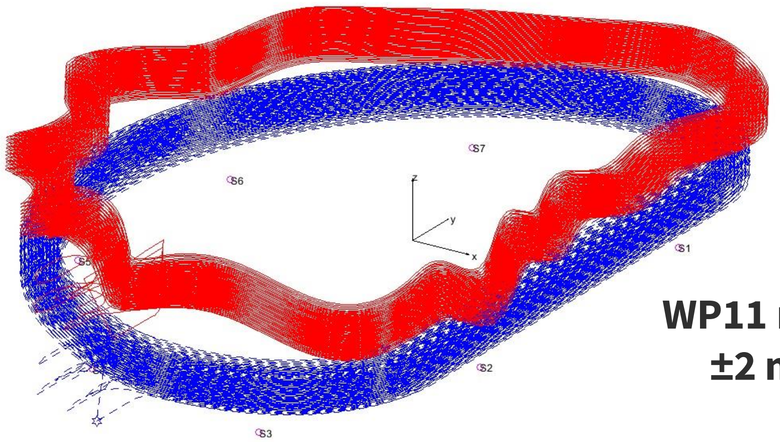

WP11 reconstruction uncertainty: ±2 mm normal, ±3 mm radial

ITER – TF Coil CCL reconstruction (5/5)

- Uncertainty of the magnetic measurement alone **< 0.5 μT** (~$3 \cdot 10^{-4}$ of full range, all frequencies)
- Estimated total measurement uncertainty generally ≤ 2 μT (~10^{-3} of full scale)
- Dominant terms: coil position error (0.8 mm RMS), coil area ($5.5 \cdot 10^{-4}$)

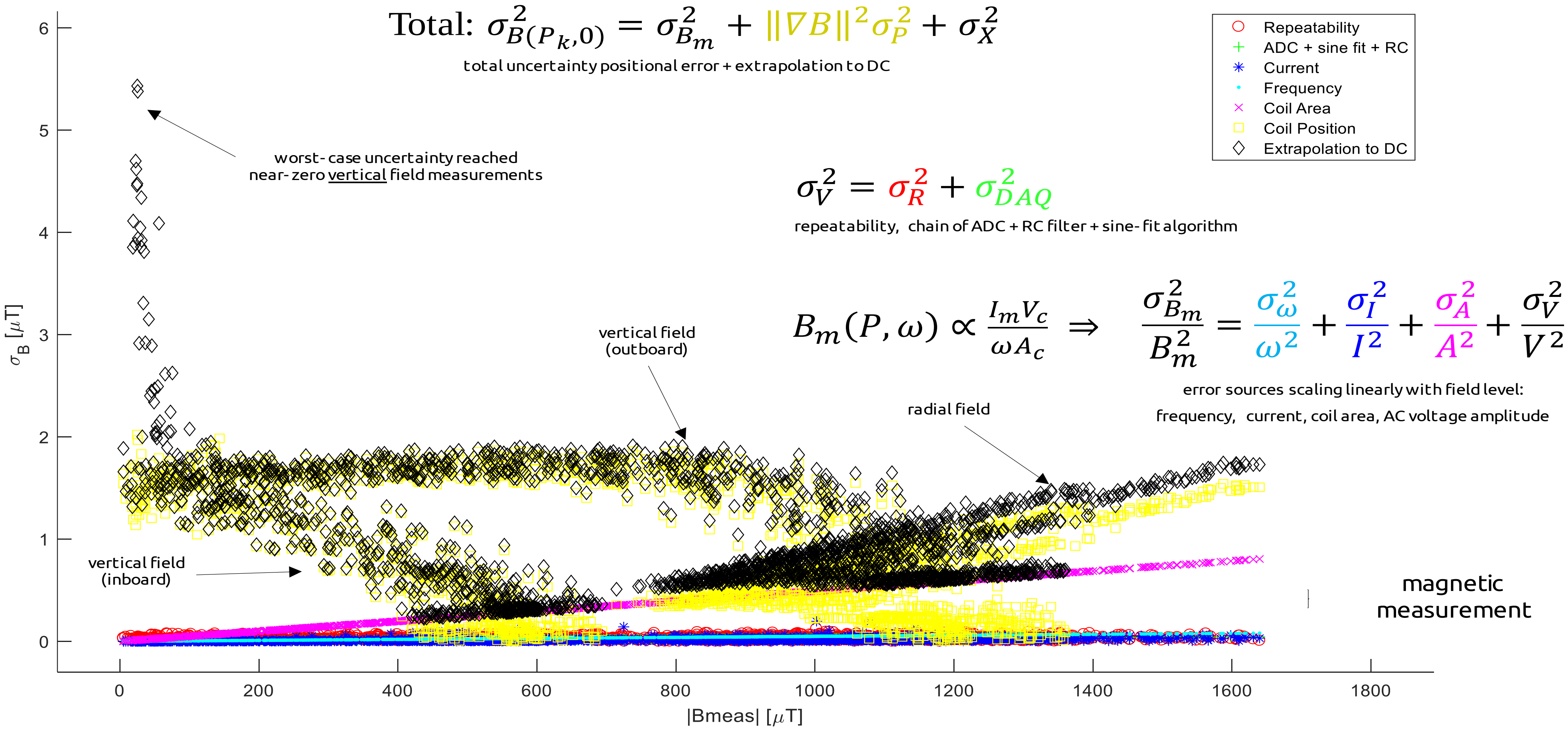

Collaboration CERN-ITER: *possible* future topics

Rad-hard Hall sensors (G. Golluccio)

- Rad-hard (**10^{18} n/m^2**) Hall probes needed at ITER (and DEMO) to correct flux loop integrator drift
- required accuracy: 4 mT up to **2.5 T**
  operating temperature **100°C** (survive baking 220° C)
- Made by Institute of Plasma Physics of the CAS, Czech Republic
- Original Bismuth doping showed ageing problem → Antimony
- ~80 units (+ a few for CERN) to be calibrated/fiducialized

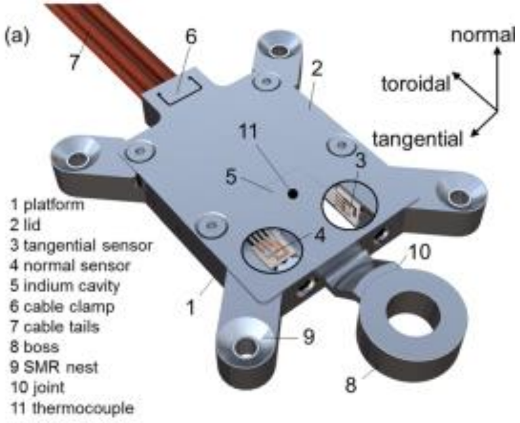

Size: 71 × 67 × 9 mm
(more room required for thermostat during linearity tests)

NMR inner vessel probes (G. Severino)

- NMR probes required during ITER construction phase to verify alignment of TF coils
- 50 µT accuracy in **ΔG/B = 0.25 m-1 @ r = 3.662 m**
  up to ~**5 T** at room temperature
- must survive baking **220° C**, rubber/water → glycerine
- Prototype proves no need of compensation n coils
- ~30 units (+ a few for CERN) to be fiducialized

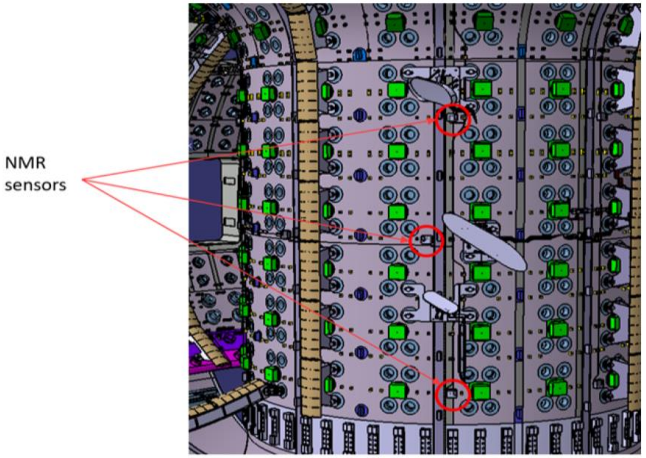

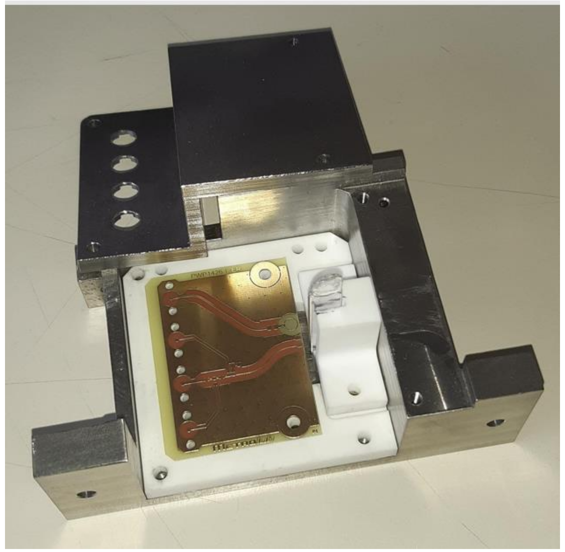

Metrolab prototype probe assembly

Instrumentation

Fluxmetric systems: rotating- and translating coils, quench antennas

Rotating coil technology overview

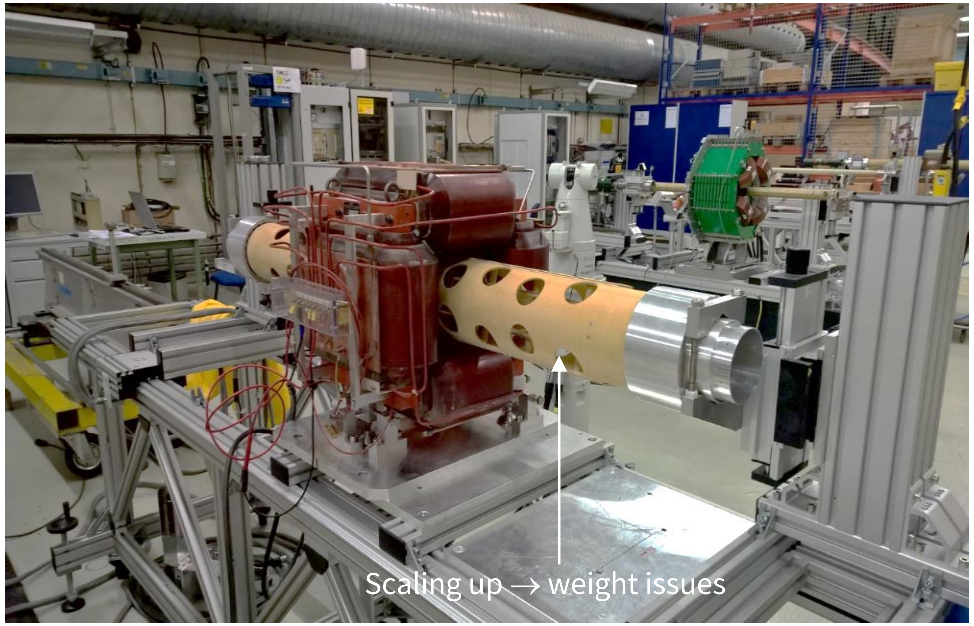

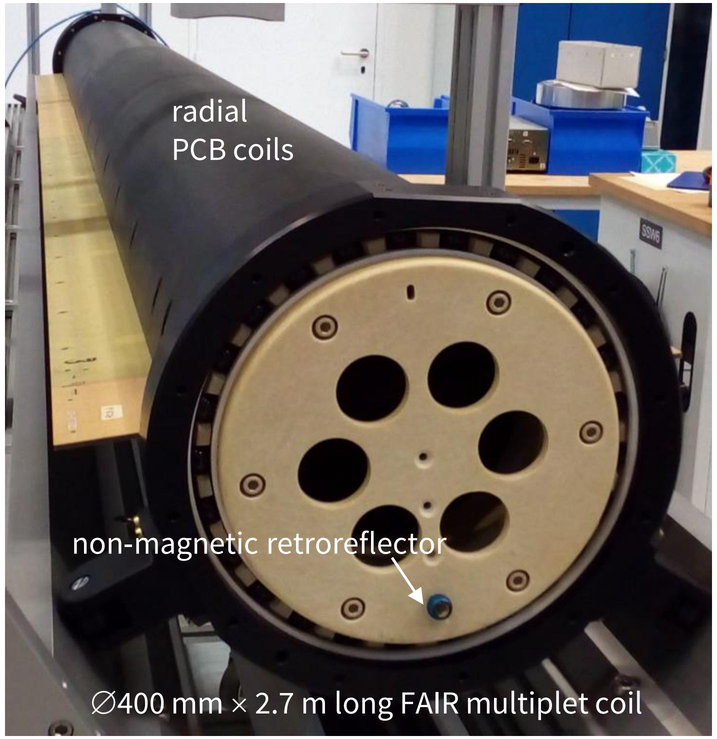

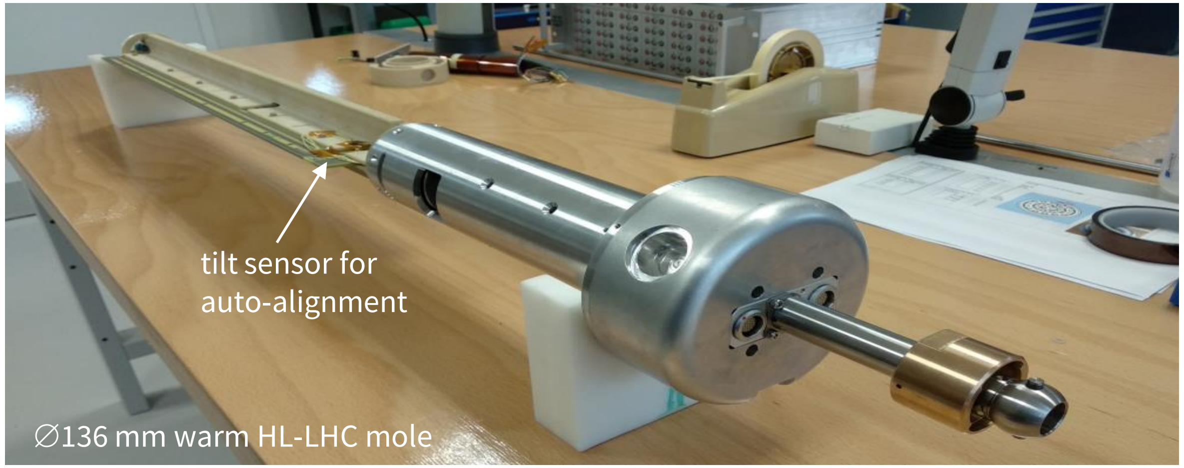

Long rotating coil shafts

- Different segment lengths and longitudinal positions to cover symmetrically all individual magnets inside HL-LHC cryoassemblies
- 13 × Ø72~109 mm, up to 16.8 m long new shafts needed for HL-LHC magnets
- Prototype Ø109 mm unit built w/ PCB coil array sandwiched between high-precision 1.4 m, 50 µm tolerance C-fiber half-shells
- Good results, but need slow down rotation above 2 T (eddy currents)
- Supply issues for the series, alternatives under study

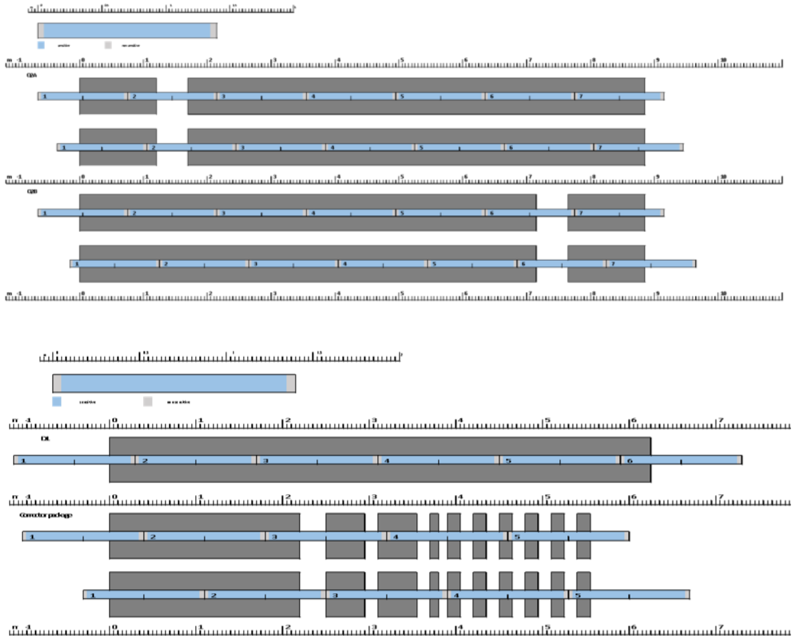

Credit: L. Fiscarelli

Project	Magnet type	N ap.	Function	Material	N	Ø (mm)	Length (m)	Weight (kg)	W/L (kg/m)
LHC	MB	2	MM/QA	ceramic	2	40	16.4	45.5	2.8
	MQ	2	MM/QA	ceramic	2	40	4.5	18	4.0
	D1	1	MM/QA	ceramic	1	40	11.4	31.5	2.8
HL-LHC	MBH	2	MM/QA	ceramic	2	40	10.6	28	2.7
	MQXF	1	QA	G10	2	109	9.0	42	4.7
	MQXF	1	QA	carbon	2	109	10.5	35	3.3
	MQXF	1	MM	G10	2	109	11.3	56	5.0
	MQXF	1	MM	carbon	1	109	10.5	35	3.3
	CP	1	MM/QA	G10	1	109	9.0	42	4.7
	D1	1	MM/QA	G10	1	109	10.5	49	4.7
	D2	2	MM/QA	G10	2	72	16.8	84	5.0

∅26 mm rotating coil for EuPRAXIA quads (INFN)

- Project goal: use standard off-the-shelf, industrially made components
- Novel **PCB-in-tube** design concept; 3D-printed Accura/Bluestone supports, DAQ acquisition of encoder signals, modular alu profile structure (final version)
- C_n repeatability ~10 ppm, absolute uncertainty of B_2 ~50 ppm, higher harmonics ~100 ppm
- Many improvements under design for the final production version

Credit: A. Lauria, R. Beltron, M. Pentella

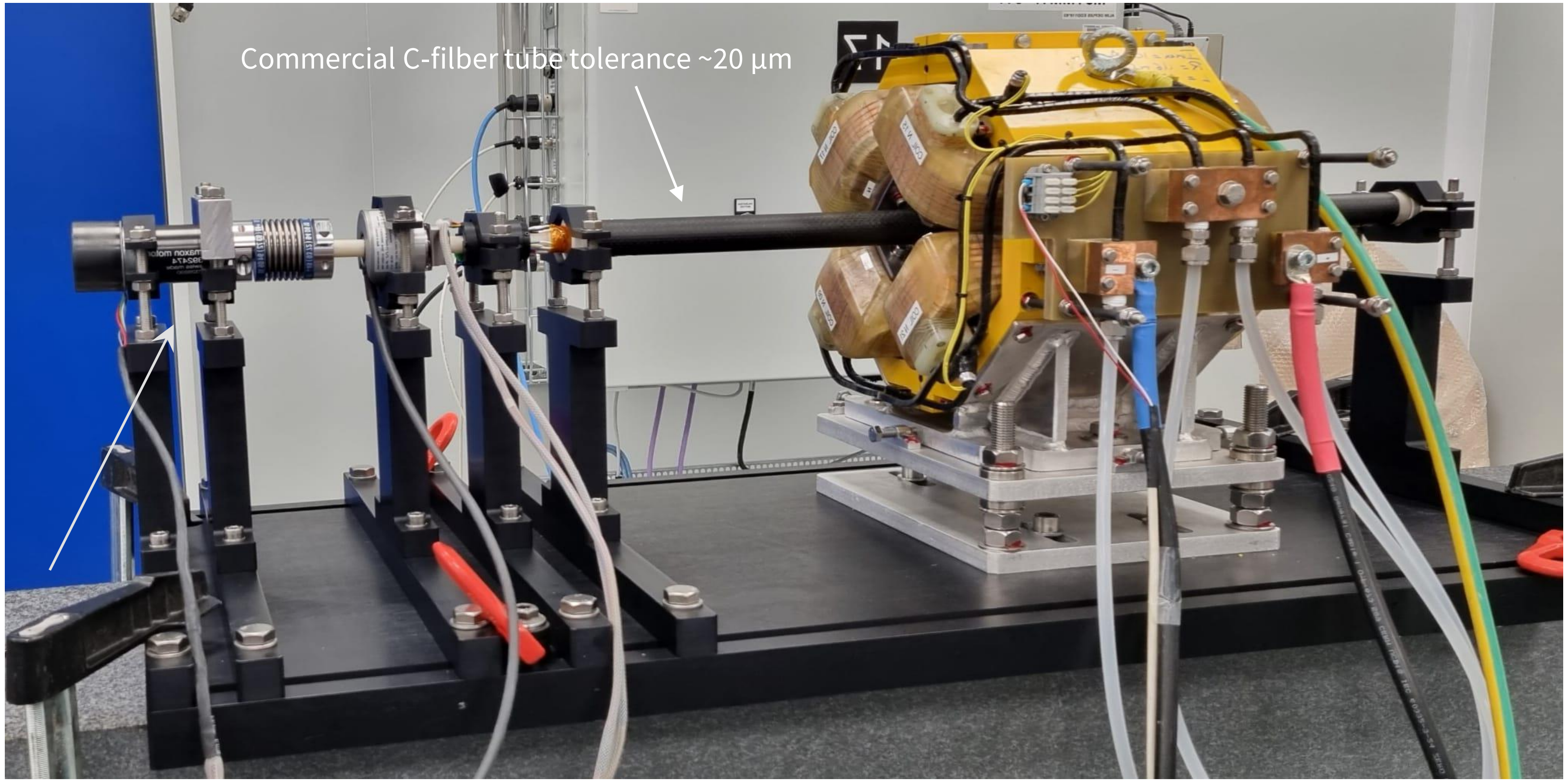

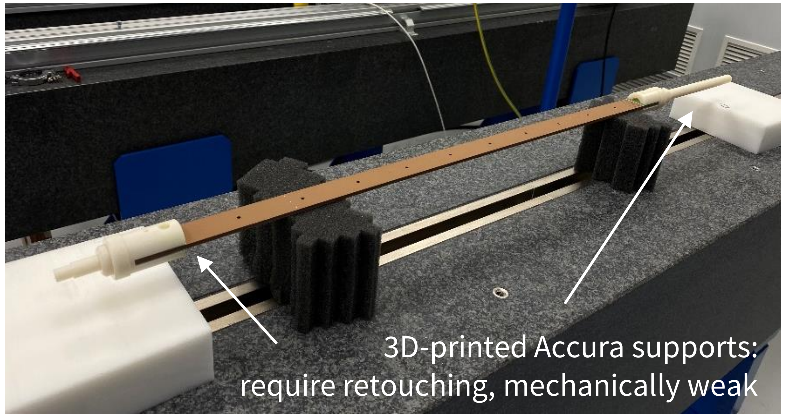

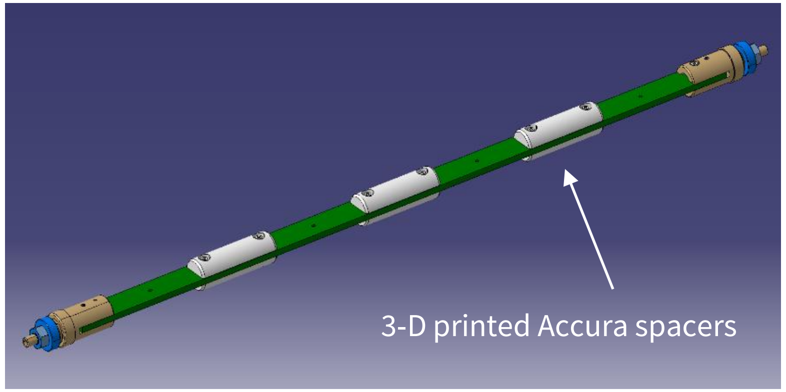

Encoderless harmonic measurement

- Can we simplify a rotating coil system by **eliminating the angular encoder** ?
- **Yes** if we assume: known average rotation speed ω_0 *or* amplitude of main field harmonic; periodic speed variation $\omega = \omega_0 + \Sigma_m \Omega_m e^{in\theta}$

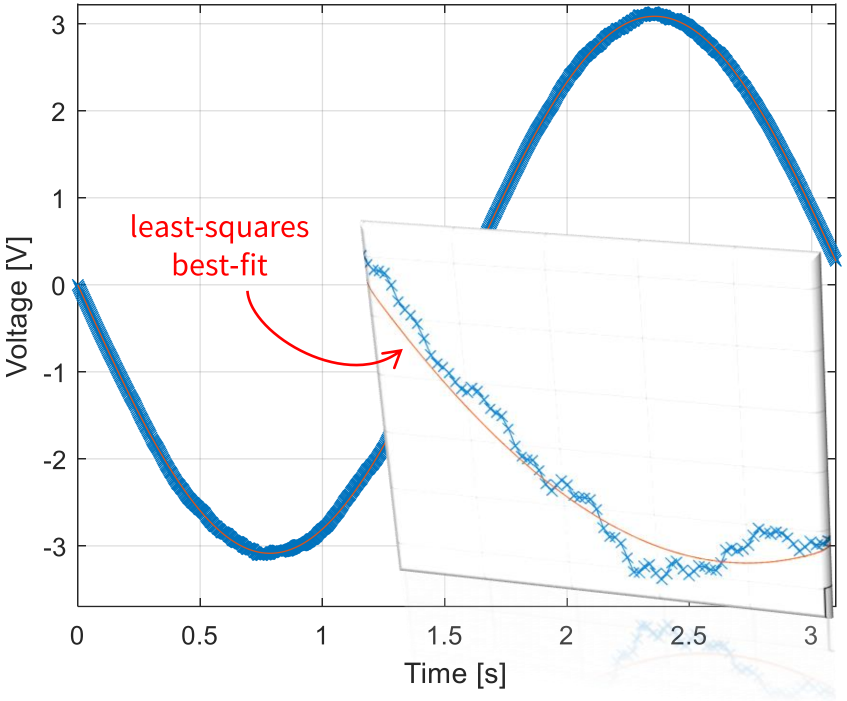

Derive $\omega(t)$ and then $\theta(t)$ from the sine wave that best-fits $V_{coil}(t)$

Credit: P. Rogacki

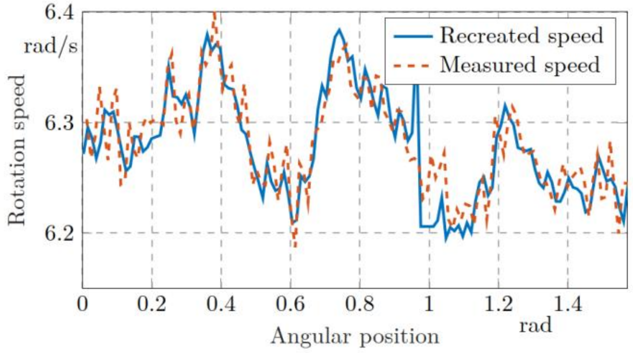

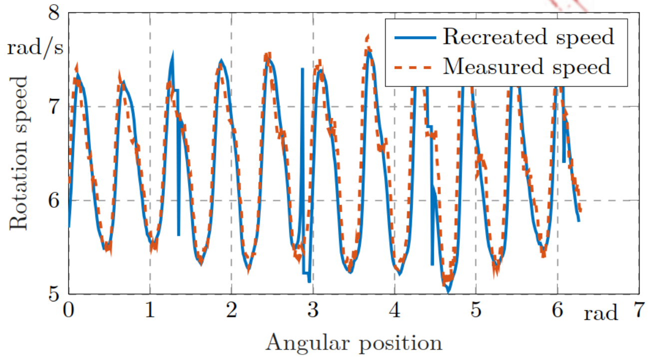

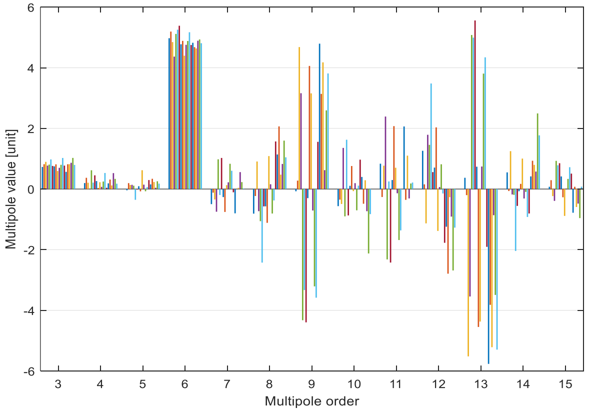

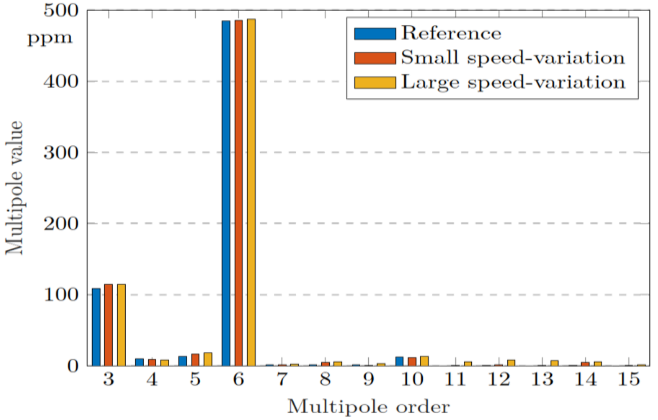

Uncorrected → Corrected harmonics

HL-LHC Quench Antenna (1/2)

- Novel design concept: **rolled-up flexi PCB**, very easy to (dis-)assemble
- Optimized for MQXF (hard-wired analog bucking)
- Improved G=100~500 acquisition electronics (analog-bucking op-amp bypassed, Z_{in} adapted to long coax capacitive load)

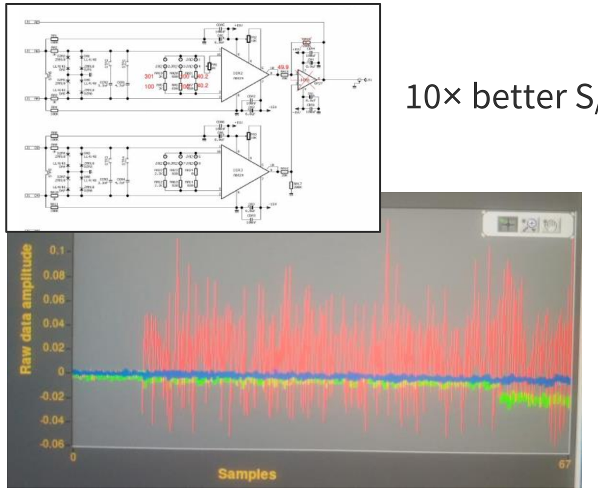

10× better S/N !!

Credit: D. Giloteaux, V. Di Capua

Credit: R. Beltron, L. Fiscarelli, J. Kaeske

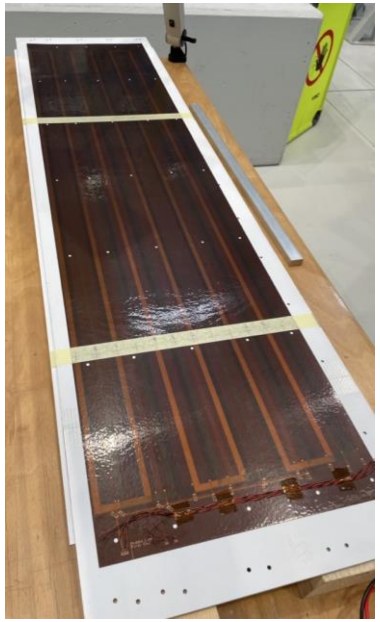

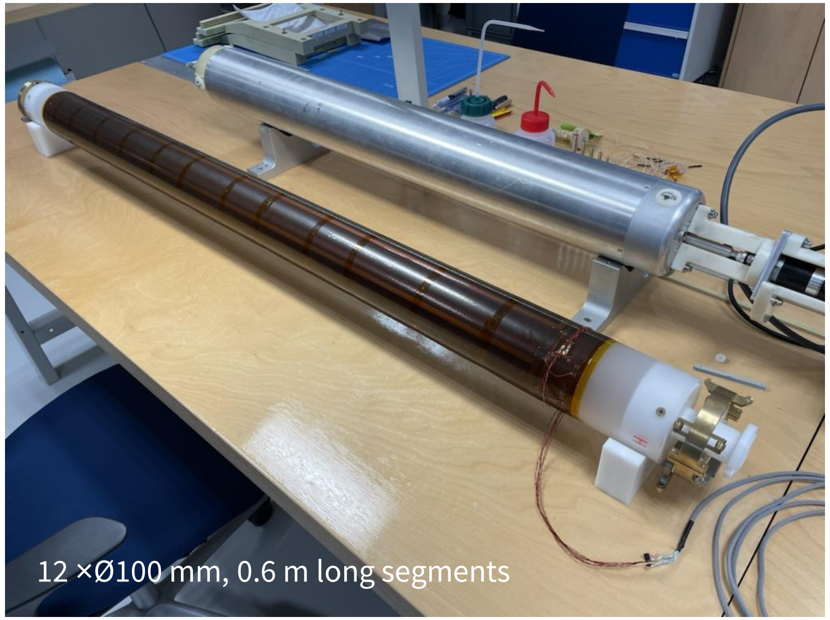

2 × double-layer flexi PCB glued together
4 × 16-turn tangential coils per layer

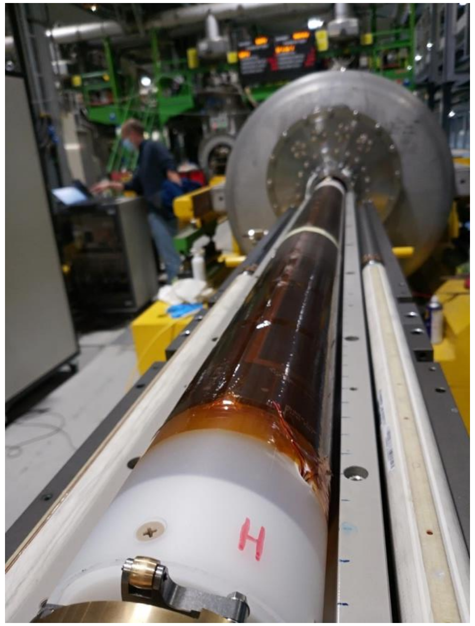

5 alignment pins foreseen,
only 1 used + Kapton tape, no glue

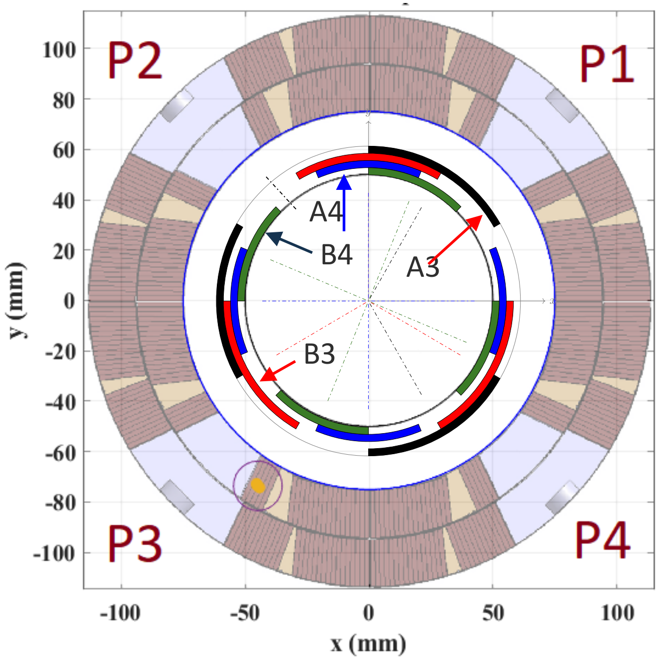

Per-layer harmonic bucking

HL-LHC Quench Antenna (2/2)

- Exceptional quality of harmonic quench signals
- Propagation speed ~700-350 m/s @ 1.9 K, ~900-500 m/s @ 4.5 K

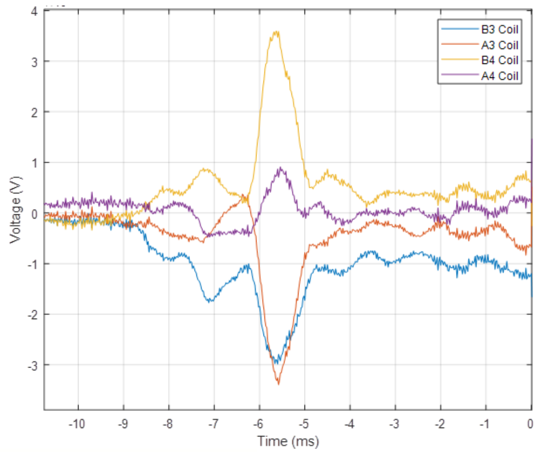

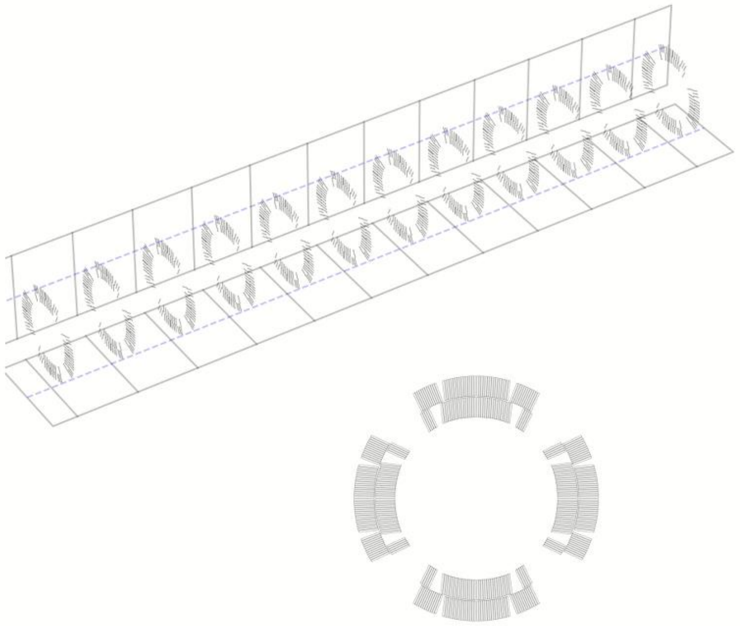

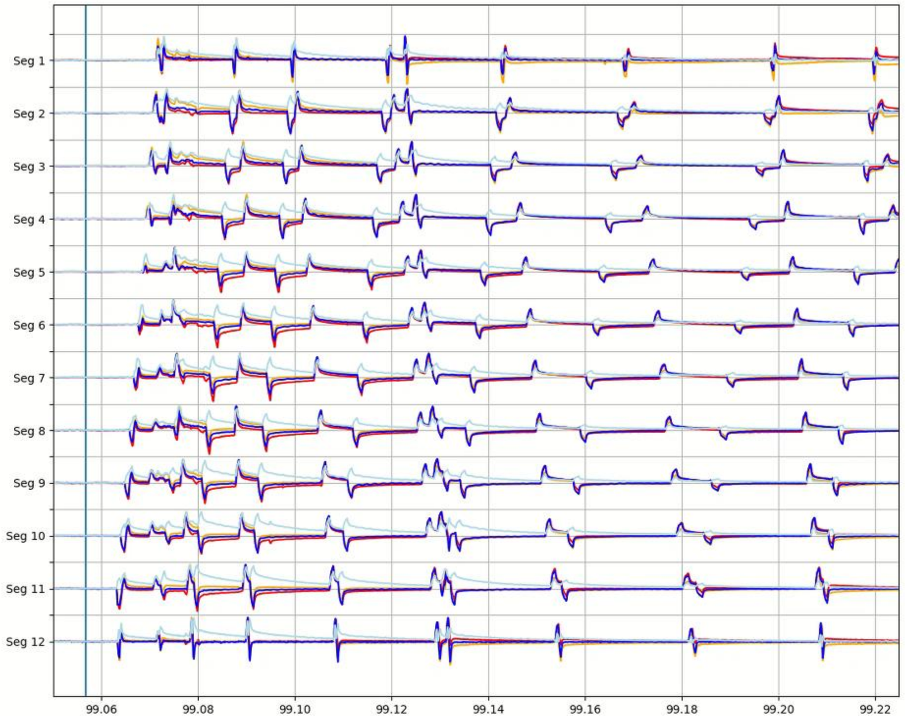

Credit: L. Fiscarelli, P. Rogacki

Translating fluxmeters (1/3)

Warm HL-LHC corrector system

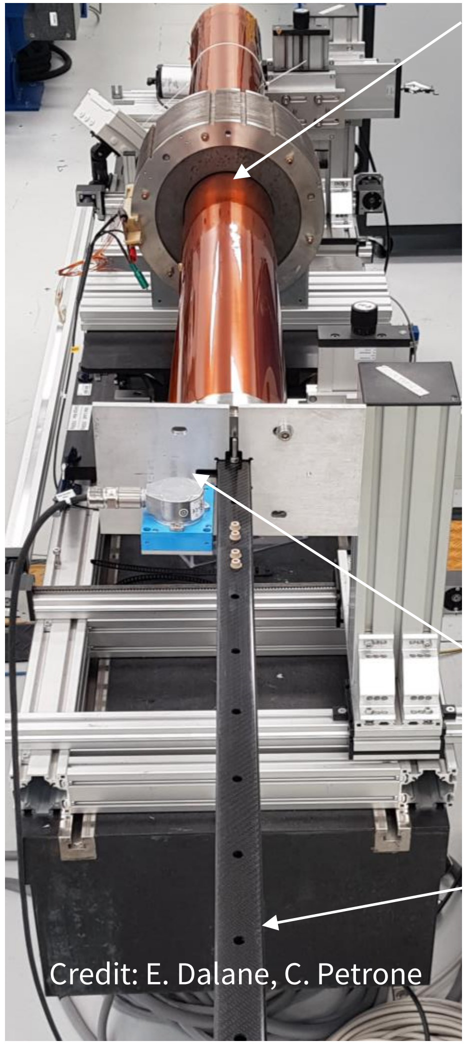

C-fiber guiding tube

12×30° PCB coils
160-turns, 16 layers, 0.06 m^2

Prototype Accura 25®
3D-printed head

Additional coil shifted by
15°/30 mm dz
pitch/yaw alignment,
azimuth refernce

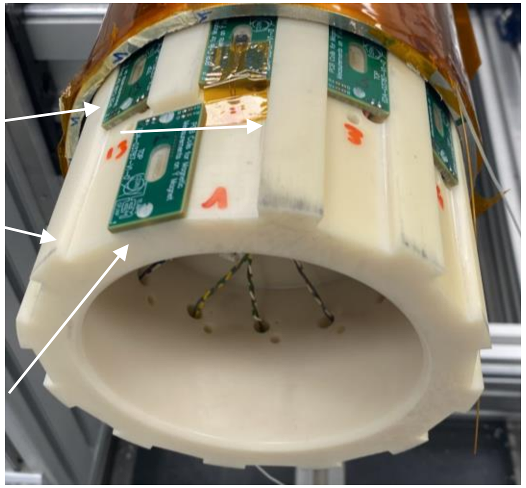

Sick® PFG08
wire draw encoder
(14 µm resolution,
300 µm reproducibility)

C-fiber moving rod
and guiding tube
(square !)

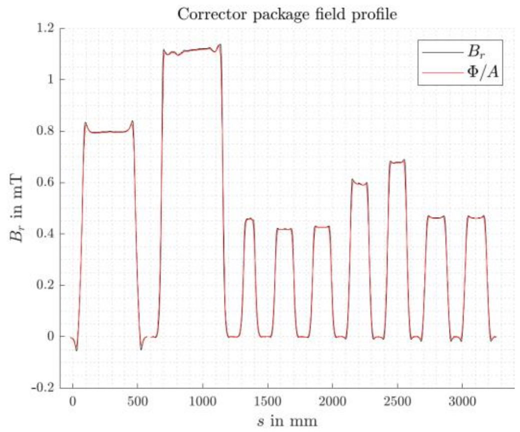

Longitudinal field profile of individual correctors in HL-LHC CP
(deconvolved with coil sensitivity kernel)
Localization accuracy << 1 mm (required)

Roto-translating fluxmeter

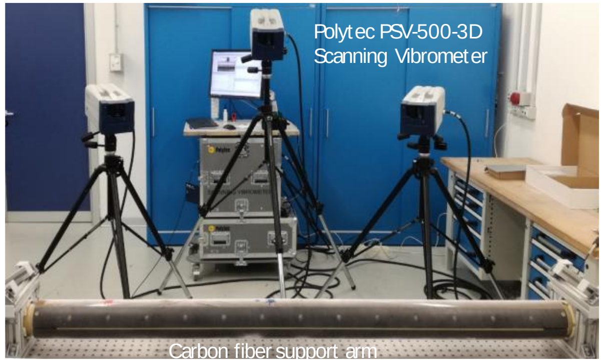

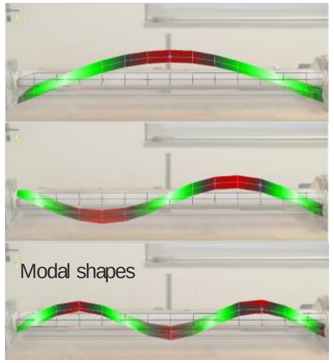

Credit: C. Petrone, S. Sorti

Translating fluxmeters (2/3)

FAIR Super-FRS dipole system

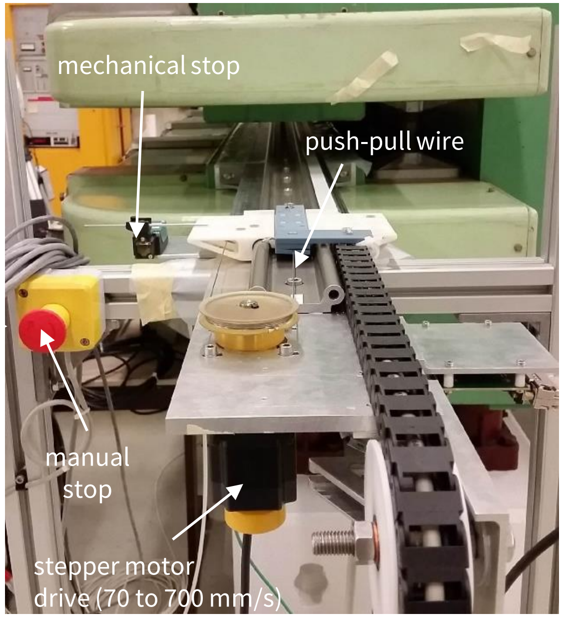

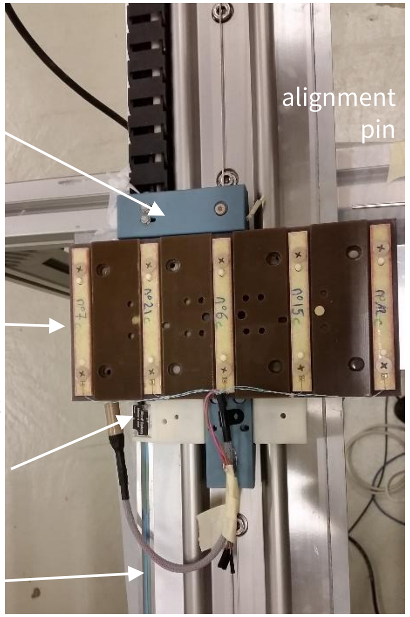

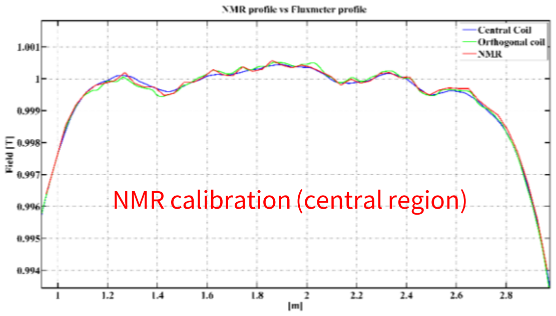

Prototype tests in MCB22 reference dipole

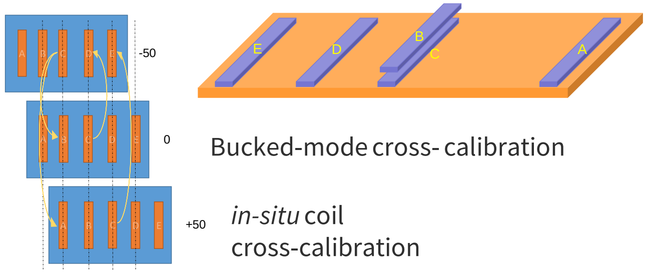

Credit: G. Golluccio, D. Caltabiano, M. Liebsch

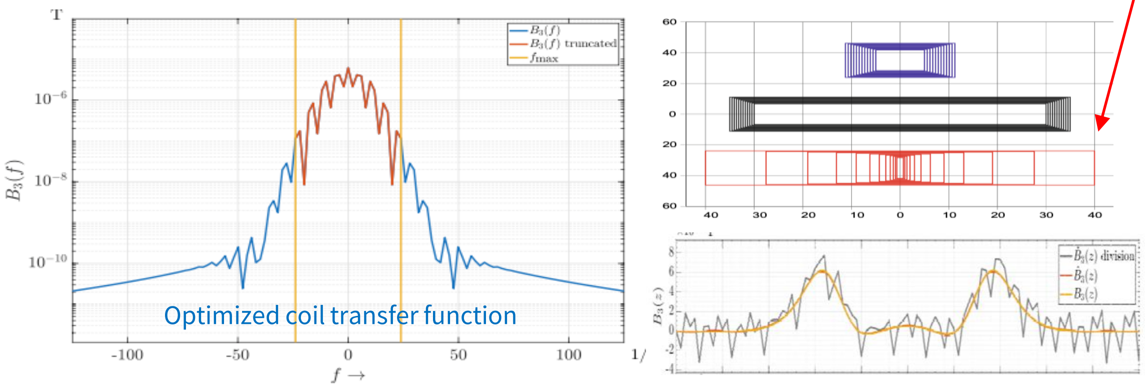

Translating Fluxmeters (3/3)

Solenoid system

- Goal: **fast in-situ measurement** of the field map/magnetic axis of 20 solenoids for the Antiproton Decelerator electron cooler
- SSW not possible (clearances, magnet cross-talk)
- Based on translating disc-shaped 8-layer PCB coil array

C Petrone, S. Russenschuck *et al.* , *"Induction-coil measurement system for normal and superconducting solenoids", IEEE Trans. on Appl. Supercond. Vol 32, n. 6 Sept 2022*

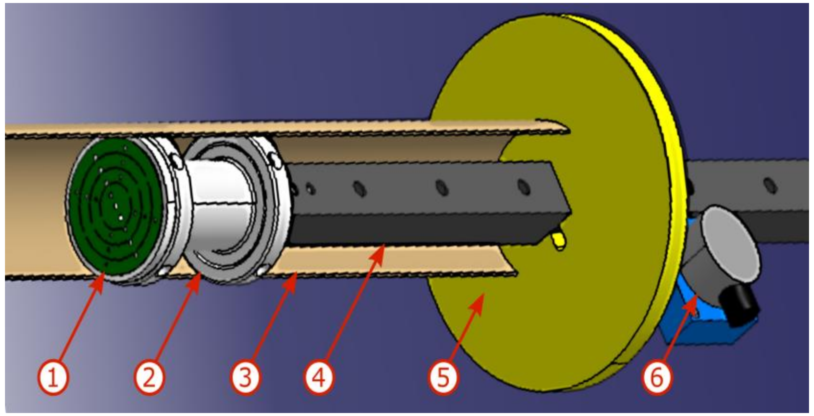

Fig. 3. Measurement system layout: (1) PCB coils, (2) Teflon PCB support and sledge, (3) guidance tube, (4) supporting arm, (5) anti-cryostat fixing plate, (6) linear encoder head.

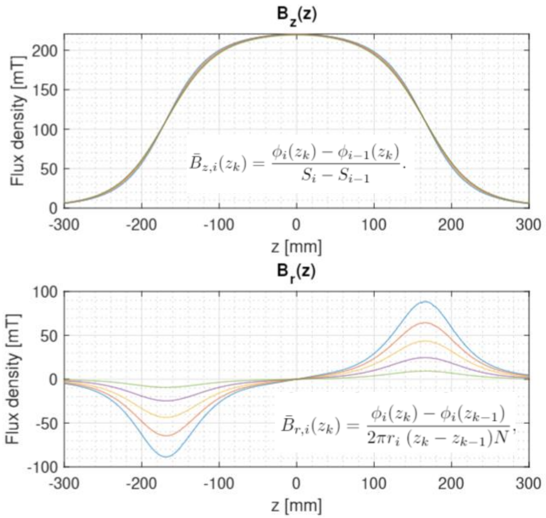

10 ppm field resolution

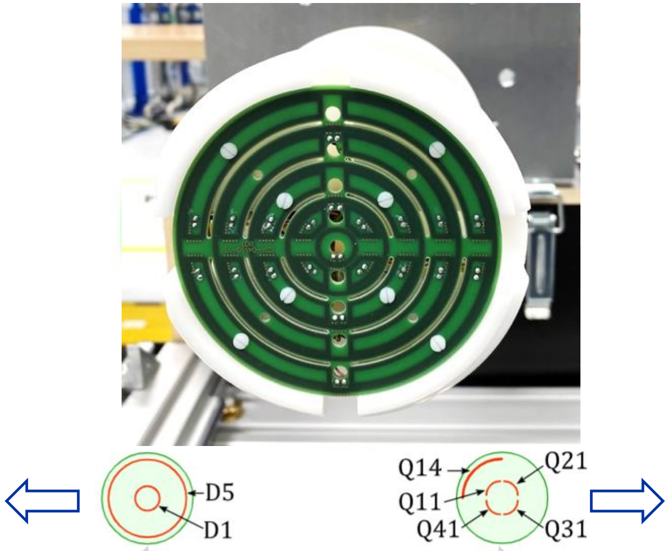

4×360° + 1 central, 6-turn concentric coils for axial and radial field profile

4×4×90°, 6-turn coils for magnetic axis localization

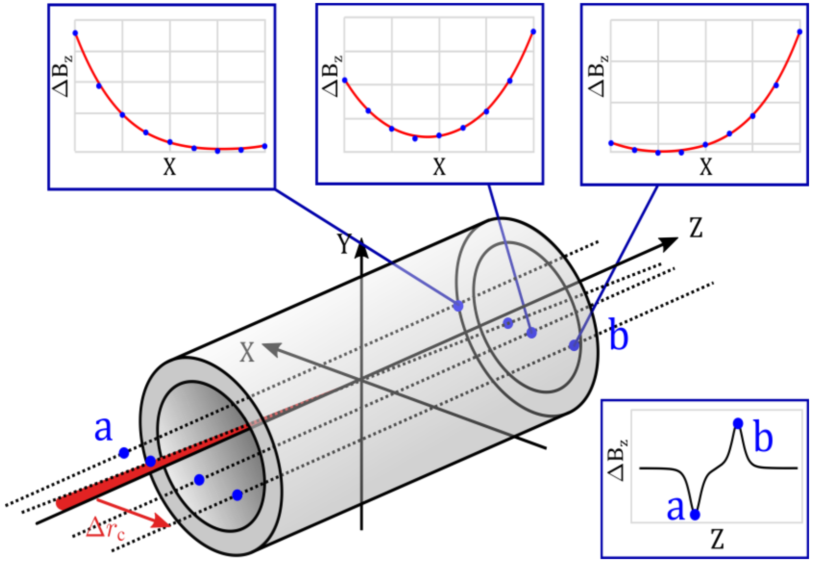

Axis defined by centers @ both end gradient peak planes

100 µm axis resolution with one pass, **50 µm** by repeating 9 passes w/ 5 mm offset

Instrumentation

Stretched-wire systems

“Curved Stretched Wire” system

- BHZ10 switching dipole issues: open-loop hysteresis (±2GeV, ±1.4GeV), L/R asymmetry
- Requirement: high precision *absolute* field integral + transversal uniformity
- Solution: a **combination of curved fixed coil + curved “stretched” wire**

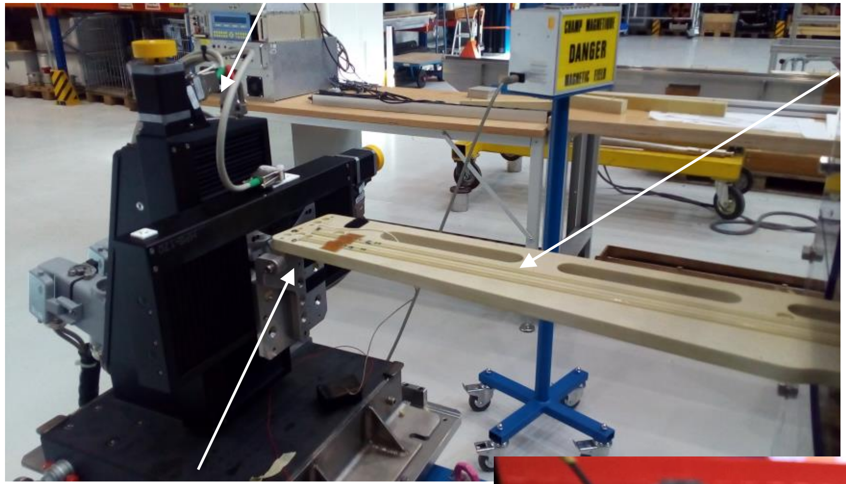

reversible G10 support for L/R beam paths
with 2 × 10 mm × 2.75 m bent coils
(no absolute calibration)
used to follow complex dynamics in fixed-coil mode

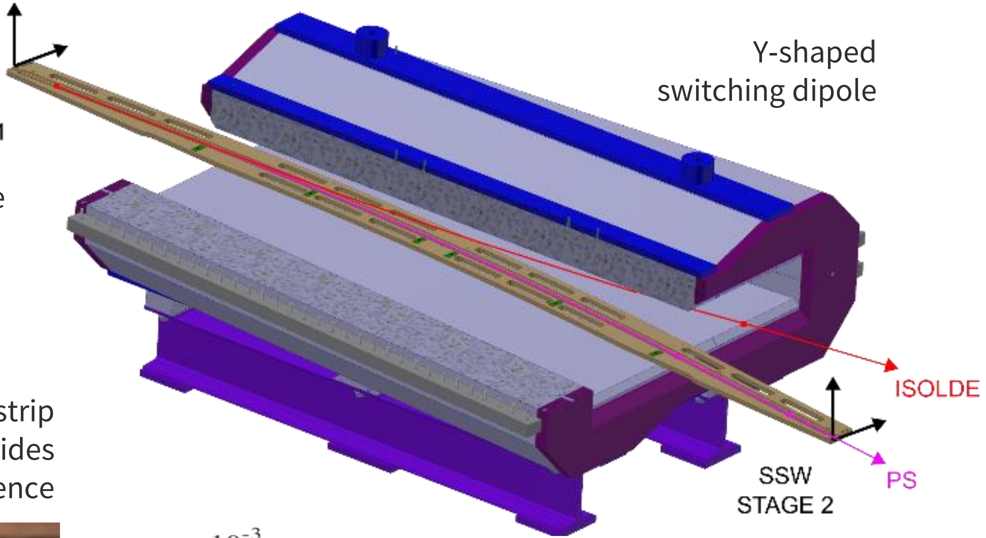

one end pivoting,
other end simply supported

1 to 3 Cu wire loops glued on FR4 strip
high-precision translation provides
the curved calibration reference

Rohacell ® PMI
structural foam support

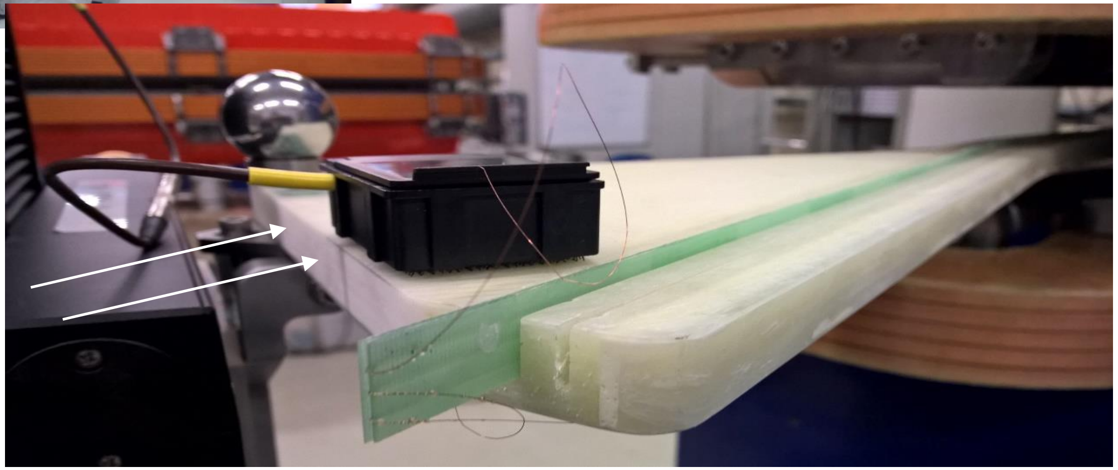

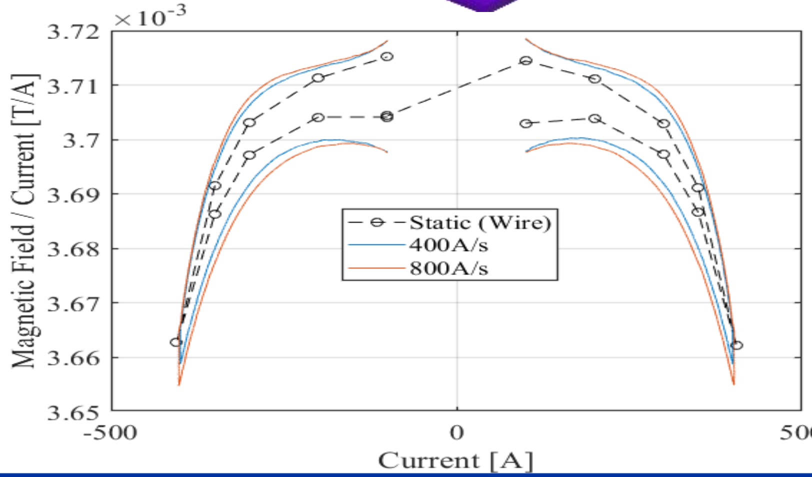

Credit: C. Petrone, S. Sorti

Single Stretched Wire systems

- 8 new systems (6 with vibrating wire functionality)
- most old FNAL hardware replaced, software based on FFMM C++ framework (see G. Deferne IMMW19)
- Reproducibility from systematic cross-calibration campaign: BdL **1.64** units, GdL **2.45** units, roll angle **0.035** mrad, axis **0.041** mm

System	Stroke	Built for	Manufacturer	Stages manufacturer	Year	In service
SSW2	150 mm	LHC	Fermilab	Newport	2003	YES
SSW3	150 mm	LHC	Fermilab	Newport	2004	YES
SSW5	150 mm	General use	CERN	PimiCos	2014	YES
SSW6	400 mm	FAIR	CERN	PimiCos	2017	YES
SSW7	50 mm	PACMAN	CERN	PimiCos	2017	YES
SSW8	150 mm	General use	CERN	PimiCos	2018	YES
SSW9	150 mm	HL-LHC	CERN	PimiCos	2019	YES
SSW10	150 mm	HL-LHC	CERN	PimiCos	2019	YES

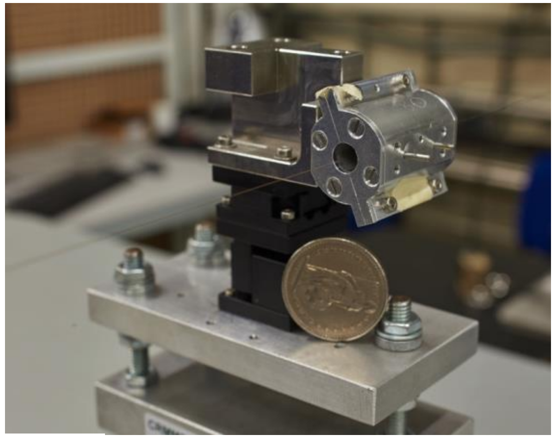

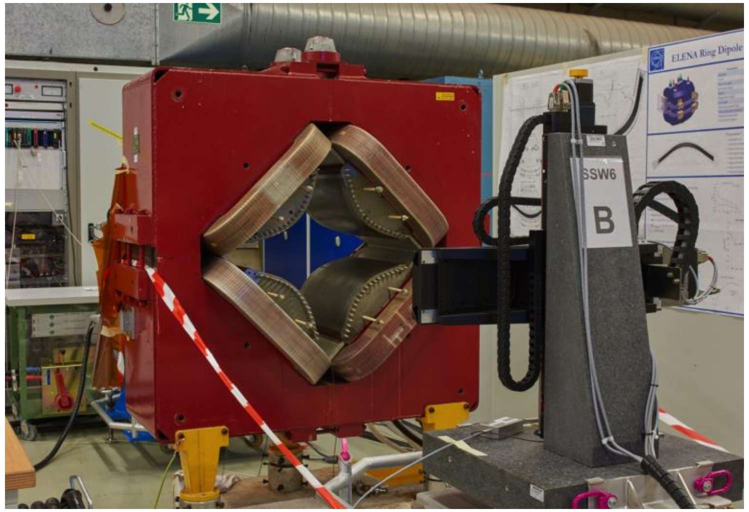

Credit: C. Petrone, G. Deferne

$$B_\eta(\eta,\psi) = \frac{1}{h_2}\sum_{n=1}^{\infty}\left(\tilde{B}_n(\eta_0)\frac{\cosh n\eta}{\cosh n\eta_0}\sin n\psi + \tilde{A}_n(\eta_0)\frac{\sinh n\eta}{\sinh n\eta_0}\cos n\psi\right),$$

$$B_\psi(\eta,\psi) = \frac{1}{h_1}\sum_{n=1}^{\infty}\left(\tilde{B}_n(\eta_0)\frac{\sinh n\eta}{\cosh n\eta_0}\cos n\psi - \tilde{A}_n(\eta_0)\frac{\cosh n\eta}{\sinh n\eta_0}\sin n\psi\right).$$

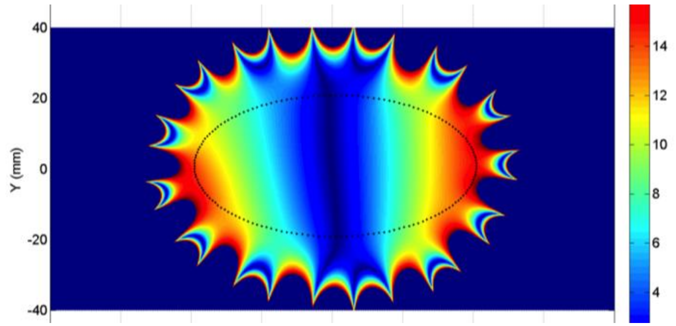

Elliptical harmonics (when needed …)

Rotating SSW: DC harmonics

- Very good results with large apertures/strong field
- Conveniently replaces ad-hoc integral coils for specific magnet
- Technique can be extended to vibrating wire for improved sensitivity (low field/small bore)

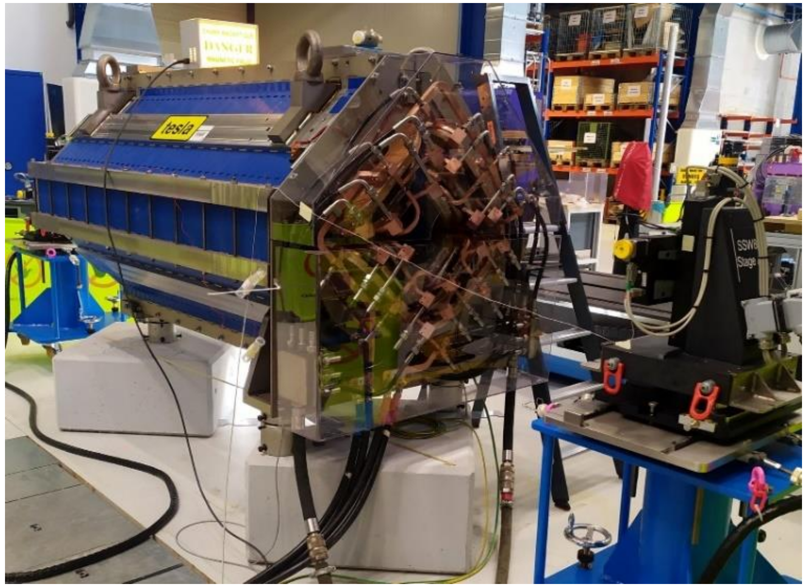

Ø140 mm quad used for cross-validation

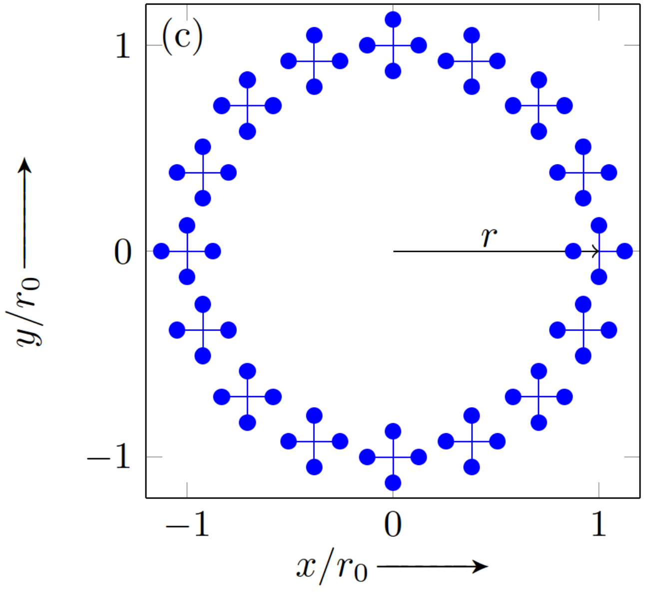

up to 128 × 3 mm × 3 mm
standard DC SSW measurements

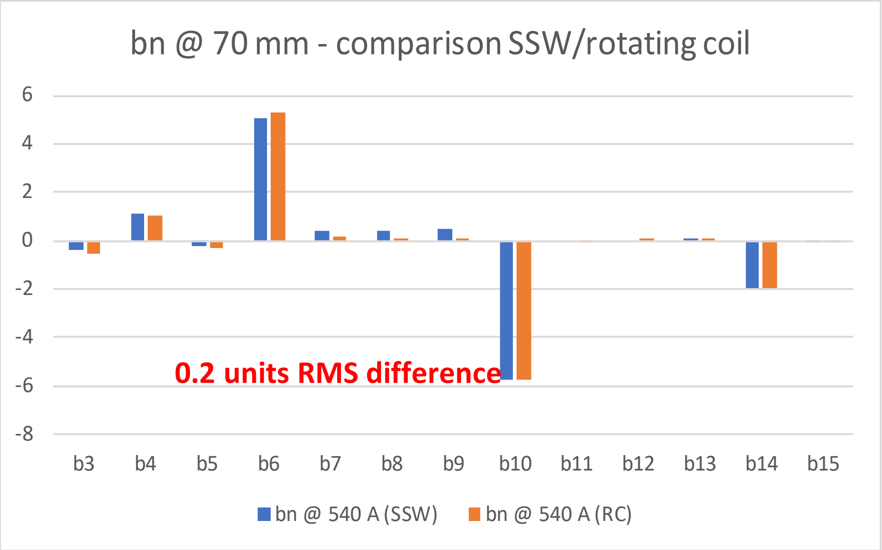

Harmonics fitted to actual flux spanned

Credit: C. Petrone

Translating SSW: AC magnet excitation

Credit: E. Dalane, C. Petrone

- Goal: warm check of axis/field direction in HL-LHC corrector package MXBXFA
- Stepwise circular wire movement to mimic a radial search coil: $\Phi_{z_n z_0} = \Phi_{z_n} - \Phi_{z_0}$
- Analytical sag correction vs. longitudinal position
- Higher harmonics not precise enough → only measured when cold

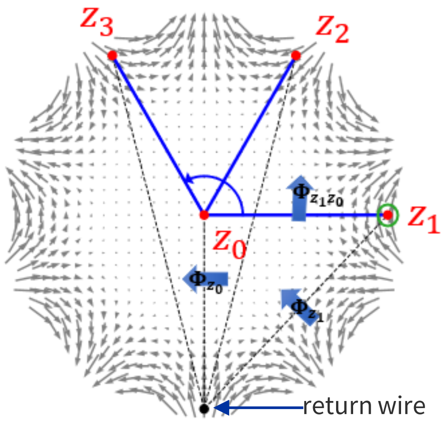

N=1 central + 256 tangential
6-second acquisitions
(oversampling)

A3 B3 A4 B4 A5 B5 A6 B6

SSW
Stage A

SSW
Stage B

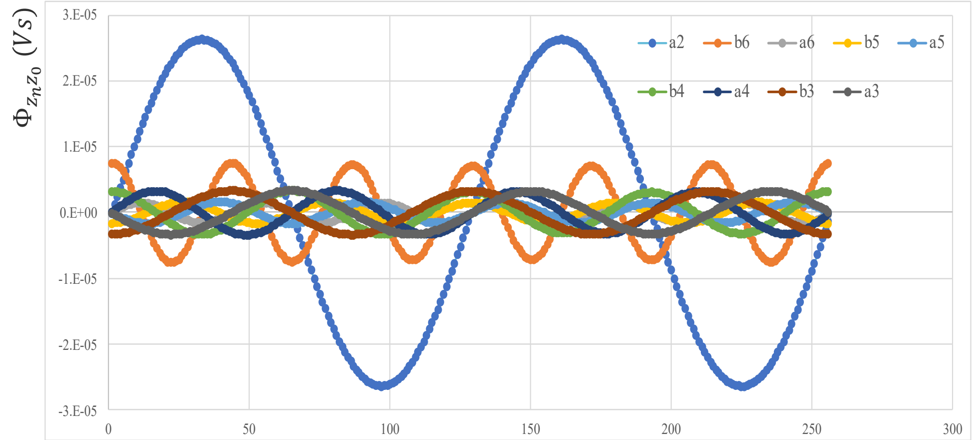

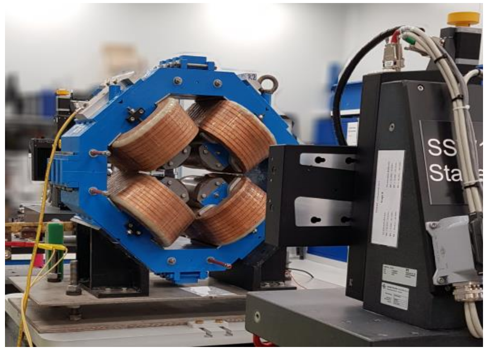

Measurement	$\Delta x \pm 3\sigma$ in μm	$\alpha_{roll} \pm 3\sigma$ in mrad
DC at 112 A	-39.6±12.87	0.086±0.079
DC at -112 A	-2.53±27.94	-0.133±0.089
DC averaged	-20.84±30.76	-0.109±0.119
AC at 18 A, 7 Hz	-19.65±5.96	-0.125±0.289

validated vs. DC-SSW on a reference quad

Magnets excited sequentially @ 19 Hz (compromise sensitivity/eddy current effects/available voltage)

Translating SSW: pulsed magnet excitation

Pulsed-mode flux integration in PS Booster main dipoles

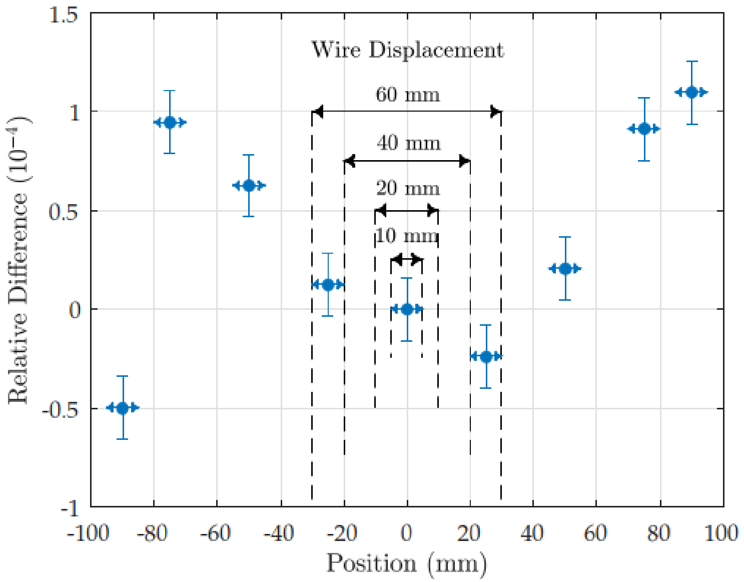

Wire offset X_2-X_1: trade-off between higher S/N and effect of B_3

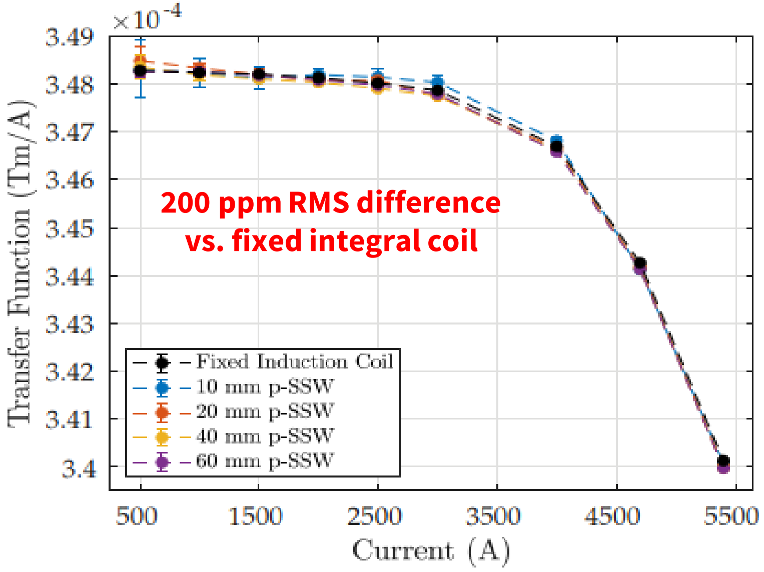

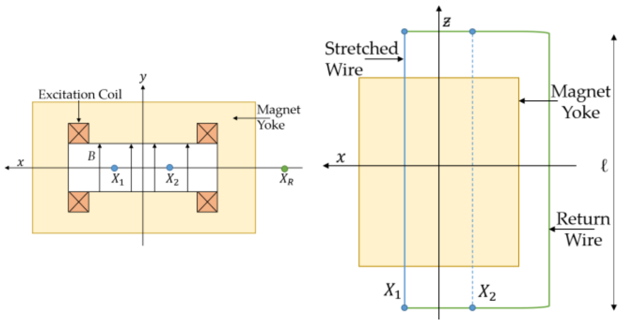

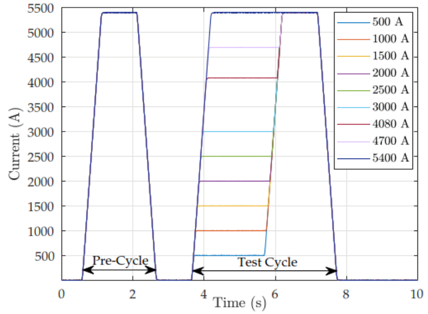

50-ppm excitation current reproducibility

Standard static SSW measurement added in to recover initial level at I_0

$$\Delta\Phi_D(X, I_0, I) = \Phi(X, I) - \Phi(X, I_0) = \int_{-\frac{\ell}{2}}^{+\frac{\ell}{2}} \int_{X_R}^{X} \left[B_y(x, z, I) - B_y(x, z, I_0)\right] dx\, dz = \int_{t_0}^{t} V_c(\tau)\, d\tau$$

Create a 1-turn virtual coil by subtracting measurements at different wire positions

$$\Phi_{\mathrm{Coil}}(X_1, X_2, I) = \Delta\Phi_S(X_1, X_2, I_0) + \Delta\Phi_D(X_1, I_0, I) - \Delta\Phi_D(X_2, I_0, I)$$

Credit: A. Parrella, J. Vella Wallbank

Instrumentation

Magnetic materials

Magnetic material properties

- Recent effort to expand instrumental range: **sample size and shape**, **permeability**, **temperature**, **dB/dt**
- Standardized procedure and software tools

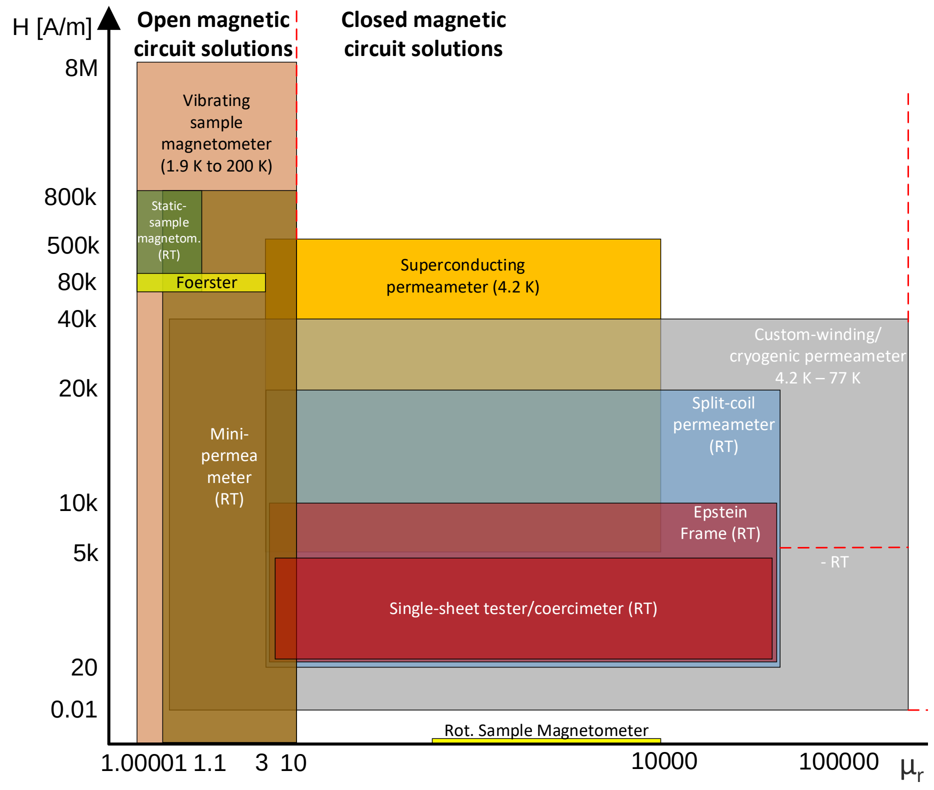

Credit: M. Pentella

Test bench	H-field range	Permeability range	Accuracy	Sample shape	Sample dimensions	T	Bandwidth	Test duration
Split-coil permeameter	20 – 24,000 A/m	1.1-15,000	<1% Magnetic Steels >5% Very low/high µ	Ring	∅ext 114 mm ∅int 105 mm H < 19 mm	RT		30 min (initial magnetization, hysteresis loop) 1 day (DC hysteresis, point-by-point method)
Custom-winding permeameter	0.01 – 6,000 A/m	1.1-500,000	1%	Ring	∅int > 70 mm ∅ext < 1.1 ∅int H > 5 mm	RT	DC-10 Hz < 50 Hz for H<10 k A/m < 1 kHz for High µ	Preparation + 30 min (initial magnetization curve, hysteresis loop) Preparation + 1 day (DC hysteresis measured by point-by-point method
Cryogenic permeameter (NC/SC)	0.01 – 24,000 A/m 800 – 500,000 A/m	1.1-500,000 (NC) 10 - 10,000 (SC)	1%	Ring	∅int > 70 mm ∅ext < 1.1 ∅int H > 5 mm	77K - 4K 4 K	DC-10 Hz	Preparation + 30 min (initial magnetization curve, hysteresis loop) Preparation + 1 day (DC hysteresis measured by point-by-point method
Epstein frame	20 – 10,000 A/m	1.1-15,000	1%	Rect. Strips	Width 30 mm L 280 ~ 320 mm	RT	DC-50 Hz	30 min (initial magnetization, hysteresis loop) 1 day (DC hysteresis, point-by-point method)
Foerster Magnetoscope	80 kA/m	1.0001-2	5%	Arbitrary	> ∅20 mm × 20 mm	RT	DC	Few seconds
Static-sample magnetometer	80 - 800 kA/m	1.00001-1.1	~50 ppm (regular geometry) 500 ppm (complex geometry)	Arbitrary CAD required for complex geometries	< 60 mm height	RT	DC	Preparation + 1 day for simple geometries Preparation + 2 days for complex geometries
Mini-permeameter	0-800 kA/m	1.001-10	0.1%	Brick	4 x 4 x 10	RT	DC	Preparation + 1 day
Vibrating sample magnetometer	0-8 MA/m	1.00001-10	10 ppm	Brick Needle	< 6 x 1 x 1.6 mm^3	1.9 - 200 K RT possible but risky	DC	Preparation + 1 day
Rotating sample magnetometer	0	-	0.1% (moment) 0.15 (angle)	Prismatic	< 150 x 150 x 150 mm^3	RT	DC	5 min

Permeameters

Split-coil permeameter

- (1967) fluxmetric setup for fast series tests
- ∅114 mm×15 mm, IEC 60404 standard samples
- 24 kA/m → saturation in magnetic steels (~2.3 T)
- pneumatic cooling, 24-bit DAQ
- 0.1% $\mu_r(H)$ accuracy on magnetic steels

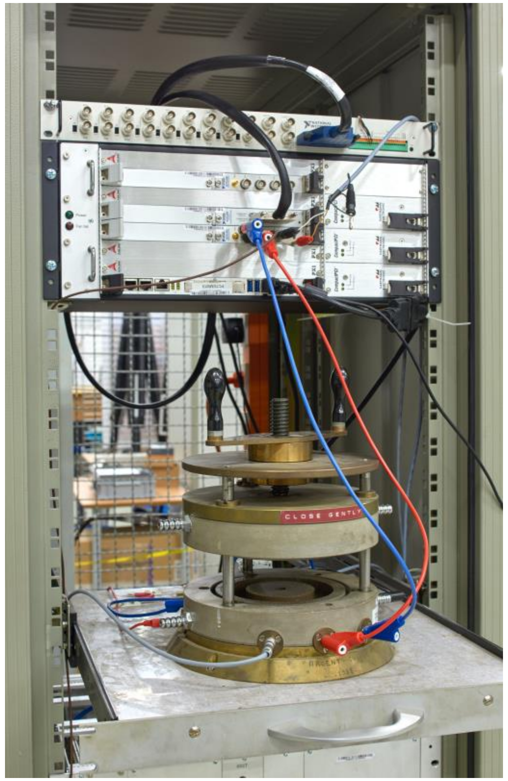

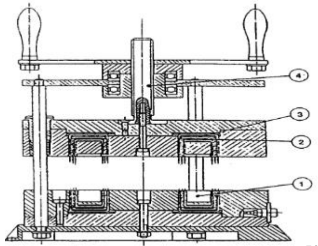

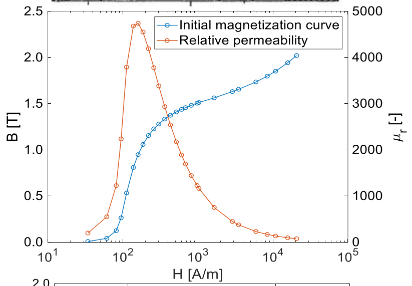

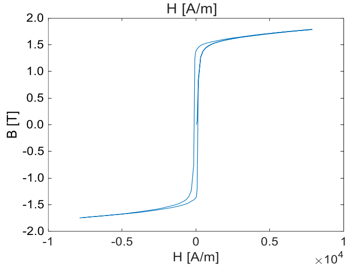

Cryogenic setup

- Samples individually machine wound in LN or LHe
- Low-ε bluestone holder (10^{-4}/K) to preserve sensing area
- 3200 NbTi turns → 500 kA/m ≈ 2.8 T (magnetic steels)

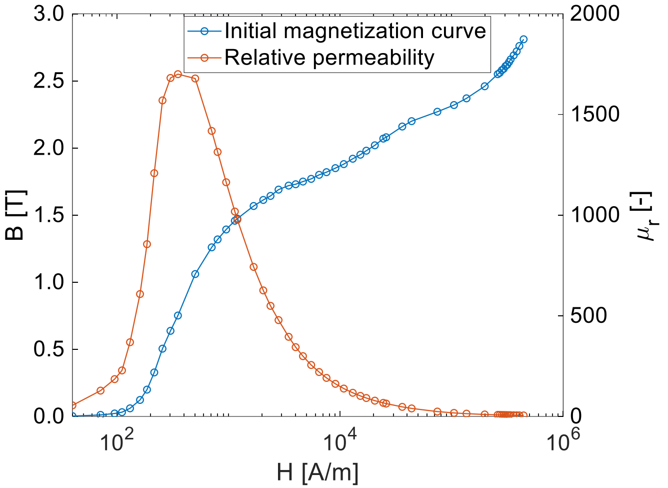

Credit: G. Montenero, A. Parrella, M. Pentella

Open-circuit, low-permeability setup

- Flux distortion method for very low permeability material (low μ_r → high field) @ room temperature
- Analytical treatment possible for simple geometries; arbitrary samples need FE simulations
- Typical accuracy 100 ppm, repeatability 10 ppm (best result: μ_r = 1.00085 of a W alloy sample, validated by vibrating sample)

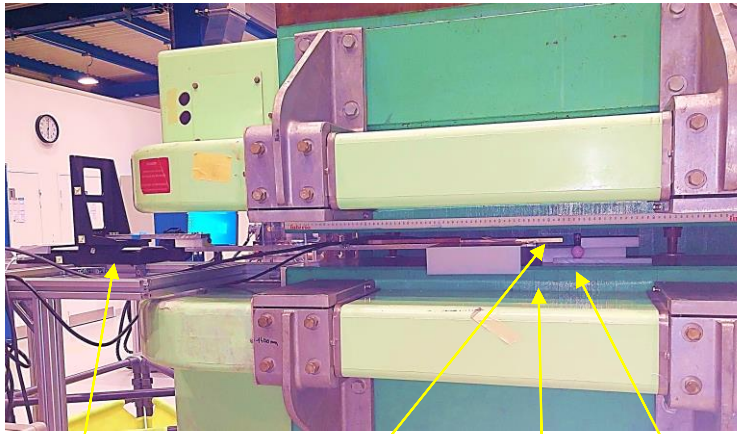

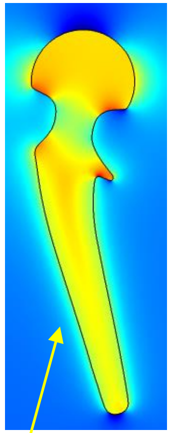

Translation stage

Moving NMR probe (5 ppm accuracy)

Sample: Ti hip prosthesis

1 T dipole, high uniformity background field

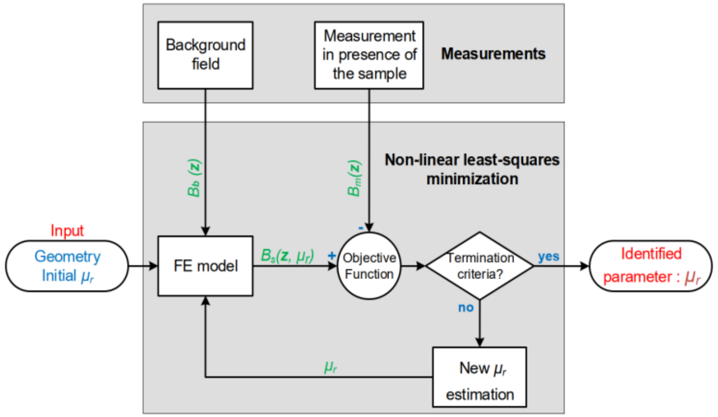

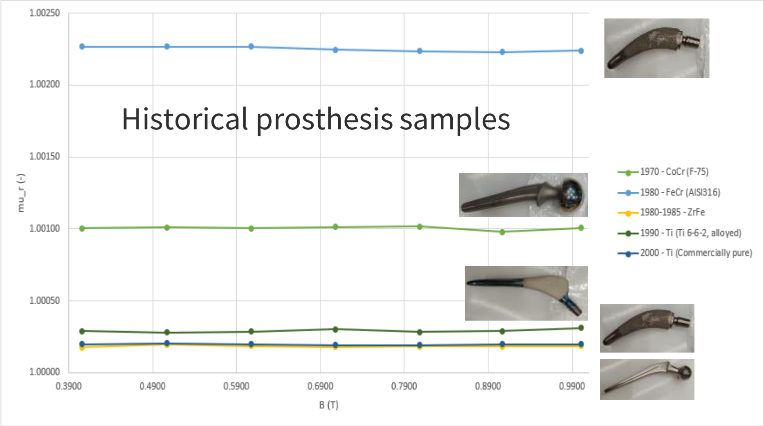

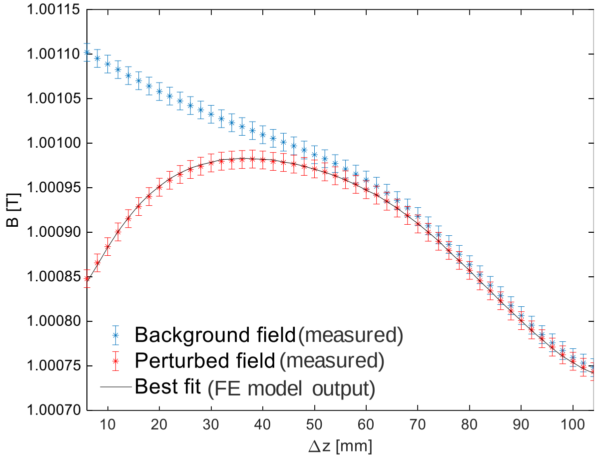

$$\frac{F_{\text{magnetic}}}{mg} = (1-\mu_r)\frac{B\nabla B}{\mu_0 g \rho}$$

Worst-case (Fe-Cr prosthesis): **μ_r=1.0023**
F_m≈mg for B∇B≈42 T/m² (i.e. ~ 20 T MRI magnet!)

Credit: M. Pentella

Instrumentation

Other systems

3D Hall probe scanner

Tapered carbon fiber arm

HE444 3D Hall sensor
(the last one !?)
8 mrad orthogonality, 0.3% non-linearity

Translation Stages by Rotondi (IT)
3 m ×1 m × 1 m stroke
100 µm accuracy @ 20 mm/s (x/y), 50 mm/s (z)

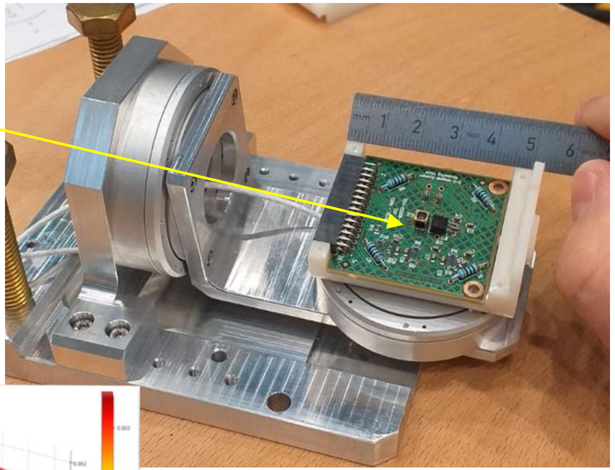

Piezo motor-based
Spherical harmonic calibrator

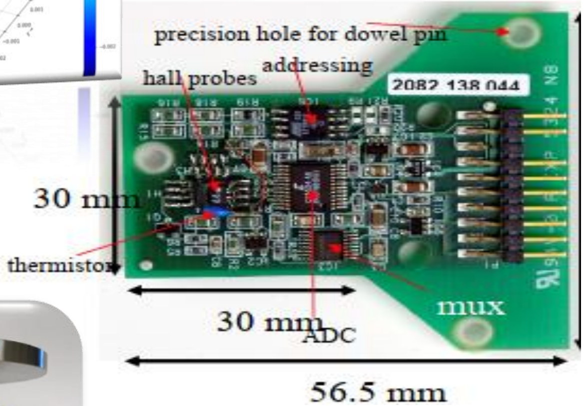

CERN/NIKHEF 3D Hall Transducer
(courtesy N. Pacifico, EP-DT)

Permanent-magnet double-cone
Fiducialization reference

Credit: M. Liebsch , S. Russenschuck, S. Sorti

Integrators

Fast Digital Integrator (PXI)

- 1 MS/s, 16-bit ADC, programmable input ampli
- FDI 3: 30+50 units in use, basis for Metrolab PDI 5025
- FDI 5: +40 dB S/N, 2 prototypes produced, project stopped

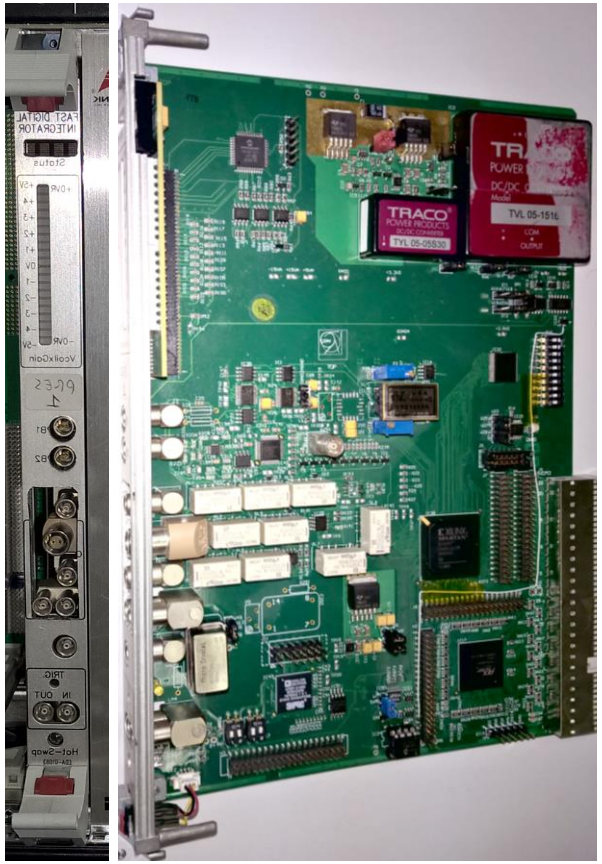

Credit: L. Fiscarelli, C. Petrone

Next-gen FMC integrator (PCIe)

- Adapted from B-train project for rotating/fixed coils
- Based on PICMG1.3 PC/Scientific Linux + CERN standard, SPEC PCIe carrier card + FPGA mezzanine
- 2 MS/s, 18-bit ADC, differential input
- Gain 0.1 to 500, input range 20 mV to 100 V
- Ratiometric correction of coil loading error (offset)
- Best-fit correction of ADC non-linearity (self-calibration)
- Remote configuration, diagnostics and data retrieval possible via FESA C++ control framework
- Prototypes under test

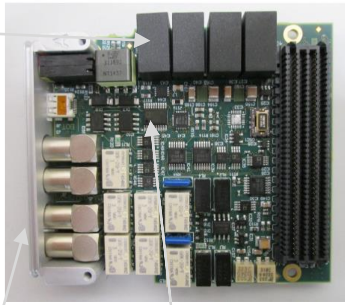

OPEN HARDWARE REPOSITORY

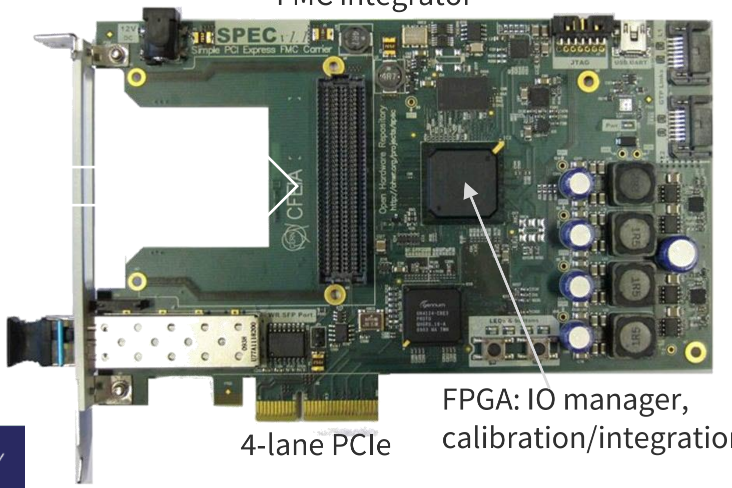

Credit: D. Giloteaux, T. Rajkumar

Paradigm Changes

Smart field mapping, hybrid modelling, sensor data fusion, machine learning

Field maps: classical approach

- Full 3D field description often needed for experimental magnets, spectrometers, certain beam line magnets (short, strongly bent, large β swings)
- Beam/particle tracing codes typically require a 3D field map, as fine as possible
- Traditional solution: deploy as many Hall probes as possible, scan the whole domain (costly !)

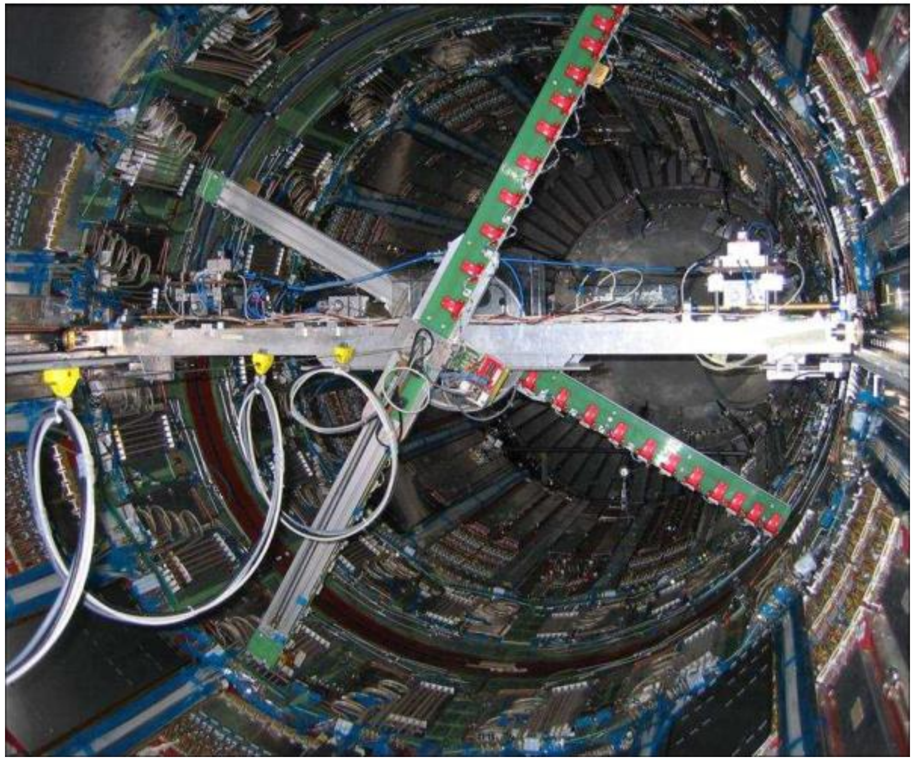

Rotating mapper for the ATLAS central solenoid (credit: F. Bergsma)

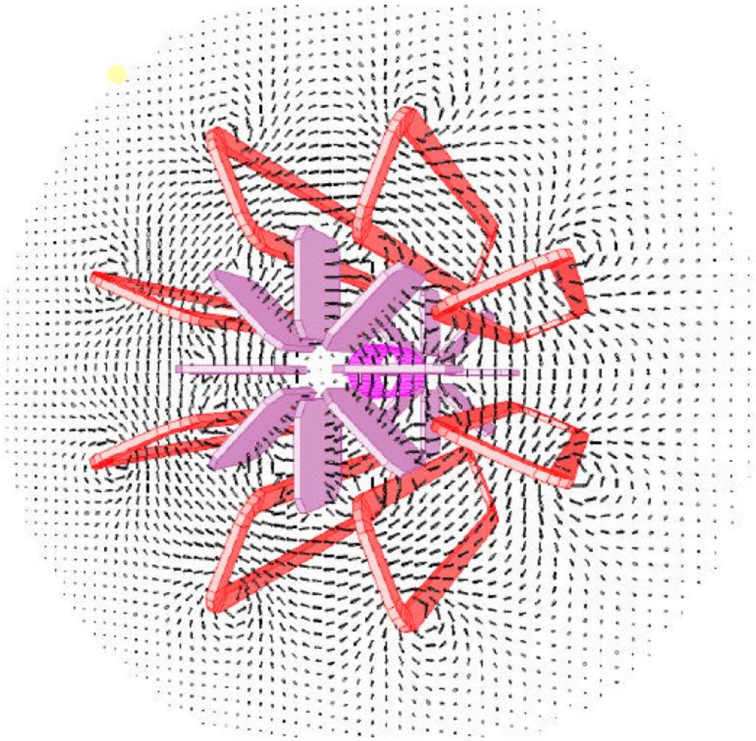

ATLAS field map

FEM/BEM processing of boundary data

- Back to Maxwell: Unique solution of Laplace equation in a source-free domain + Neumann (normal field) or Dirichlet (tangential) boundary conditions (if: simply connected domain, smooth boundary)
- **Reduce problem dimensionality**: scan only the boundary, fit a BEM model to get interior values at arbitrary resolution (no volume mesh required !)

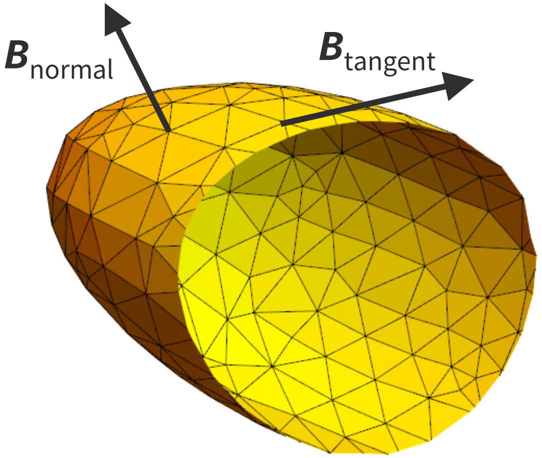

- Back to Maxwell: Maximum Principle: extremal values always on the boundary → metrological advantage of interpolating the interior

2D example, cylindrical symmetry: Measurement uncertainty at $|z|=r_0$

$$B_n = C_n \left(\frac{z}{r_0}\right)^{n-1} \Rightarrow \sigma(B_n(z)) = \sigma_B \left(\frac{z}{r_0}\right)^{n-1}$$

- R&D challenges: automated meshing and setup of BEM model; hybrid boundary conditions (e.g. integrals from flux measurements); incorporate arbitrarily scattered/multiple/interior points

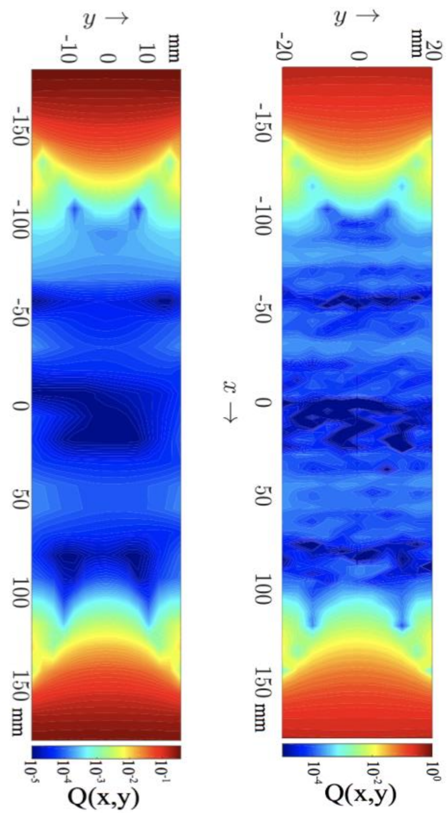

BEM reconstruction

Full grid

Credit: M. Liebsch

Hybrid modelling : traditional iterative approach

Numerical models

- Arbitrary parameter range, precision of results
- Best at relative differences and changes
- Automated parametric analysis
- Object does not need to exist !
- Errors: modeling, approximation, discretization, numerical

Measurements

- Practical limitations: sensors, power converters …
- Best at absolute results
- Cost scales with number of test cases
- Object “as built”
- Systematic and random errors: capture and readout noise, calibration, quantization, numerical post-processing

Requirements

design

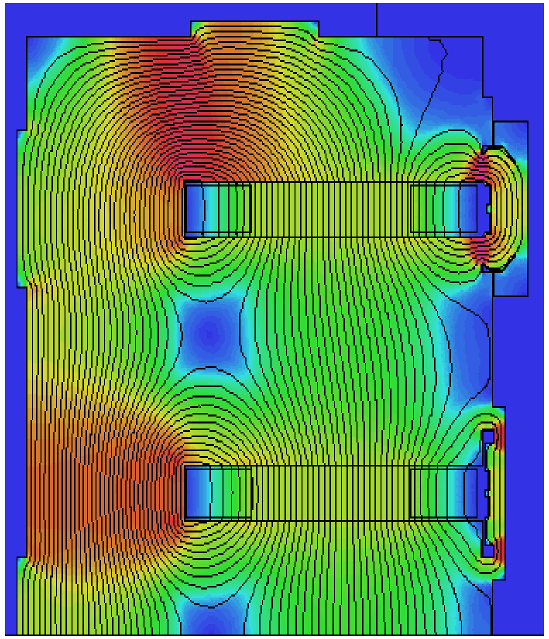

manufacturing

(mech. tolerances, material properties, excitation history …)

4-ring bending dipole of CERN PS Booster

testing

Performance characterization

prototype feedback

Hybrid modelling: data-driven digital Twins

- Combine optimally the strong points of computer modeling and measurement
- Formalize and automate the comparison of computed and measured quantities
- Different possibilities: build the instrument in the Twin, feed back measurement in the FE model (inverse field problem) …
- Simple example: ISOLDE 90° spectrometer

Parameters $\boldsymbol{p}$
(h, μ_r)

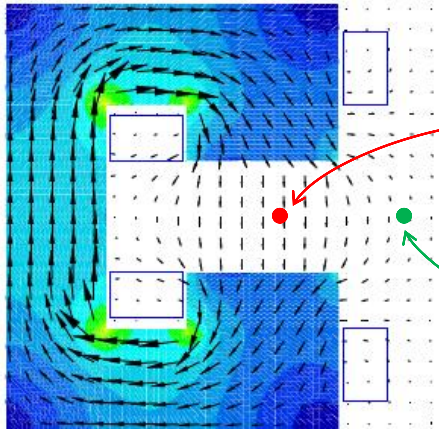

… and we want the field here …

… but we can only measure B_j there !

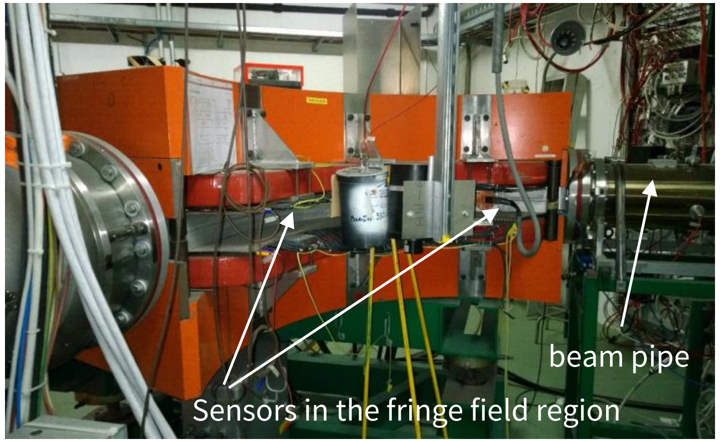

Measurement uncertainty
σ_B

Bayesian priors
(h_0, σ_h)
(μ_{r0}, σ_μ)

We don't know well these …

computation

measurement

$$\chi^2(\boldsymbol{p}) = \sum_k \frac{(p_k - p_{k0})^2}{\sigma_k^2} + \sum_j \frac{\left(B_j^{\text{comp}}(\boldsymbol{p}) - B_j^{\text{meas}}\right)^2}{\sigma_B^2}$$

Minimization w.r.t. $\boldsymbol{p}$

$$J = \frac{\partial B_j}{\partial \boldsymbol{p}}^{\text{comp}}, \qquad H = \frac{\partial^2 B_j}{\partial \boldsymbol{p}^2}^{\text{comp}}$$

Indications for experiment design

Sensor fusion: induction coils + Hall probes

- Trend: combine both sensors on same PCB, whenever possible
- Trivial applications: magnetic length, center field, fringe profiles
- Real interest: cross-calibrate by exploiting coil's linearity, Hall sensor's absence of drift

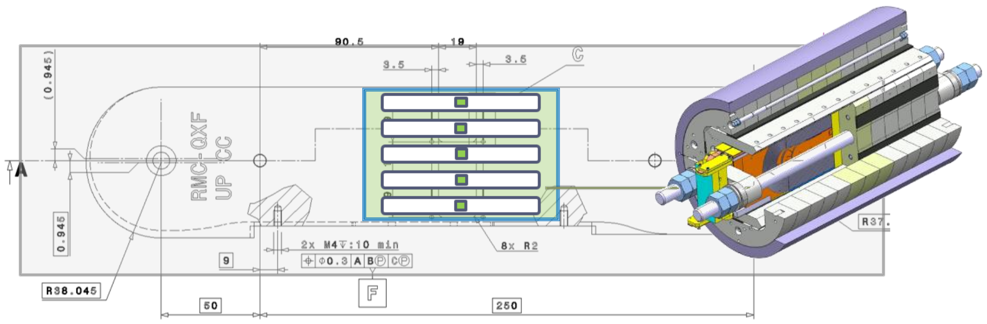

Nb$_3$Sn racetrack model coils

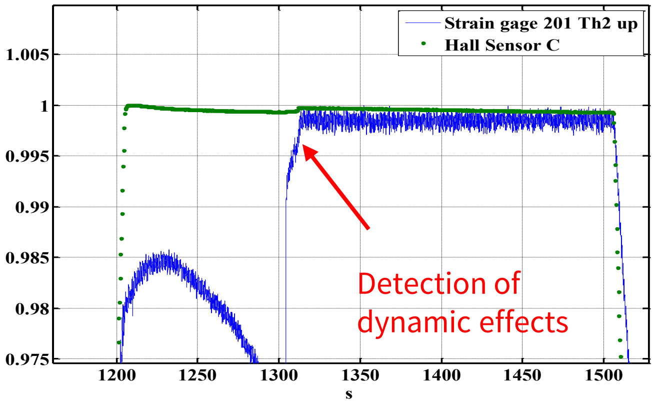

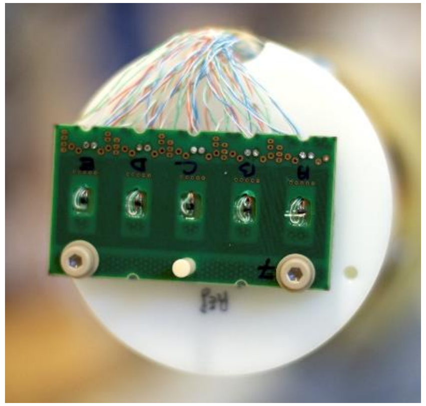

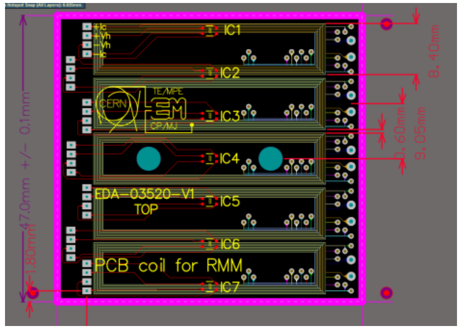

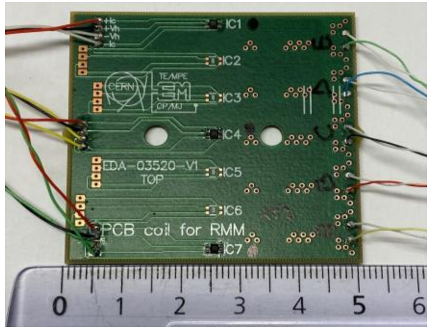

3× aerospace-grade LakeShore HGT 2101 Hall probes (highly nonlinear!)

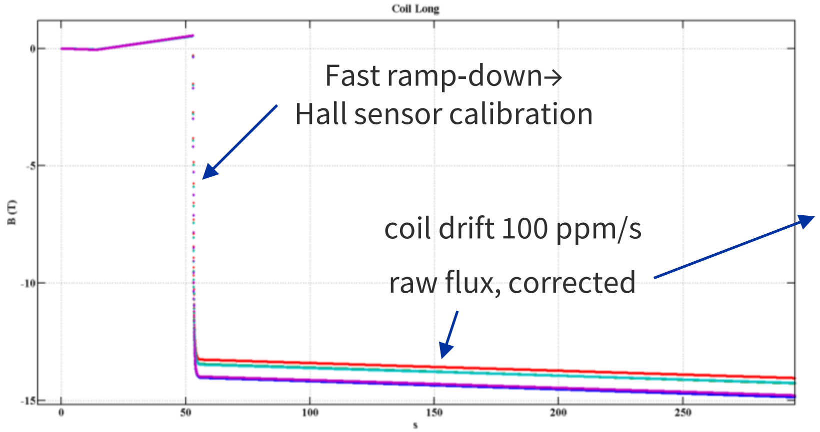

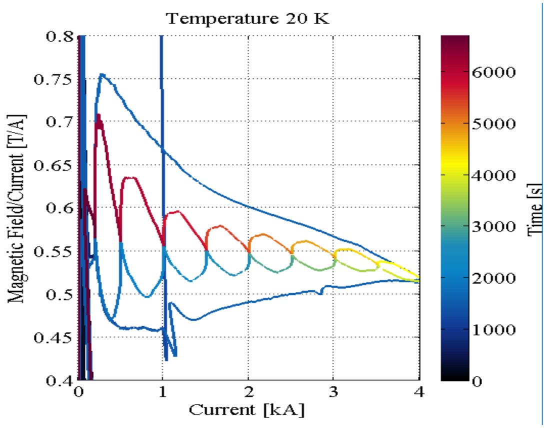

Credit: L. Fiscarelli, C. Petrone

Sensor fusion: Kalman-based integrator drift correction

- Problem: fixed-coil voltage integrator drift
- Kalman filtering: optimal estimation of the field in the presence of model (voltage offset V0) + measurement noise
- Combining coil/Hall probe → <u>three orders of magnitude</u> improvement

Field = hidden state   Coil voltage = input variable

State-space model $$x_k = B_k = B_{k-1} + \frac{1}{A_c}\frac{(v_k + v_{k-1})}{2}T_s$$

Case I: measurement = Hall probe

$$z_k = B_{H,k} = B_k + q_k$$

Case II: measurement = excitation current

$$z_k = \frac{I_k}{g} + q_k$$

Arepoc HHP-NP 2067 Hall Probe

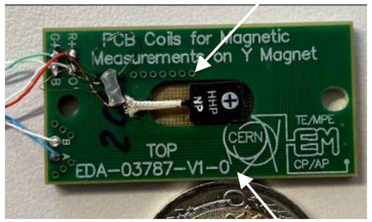

594 cm^2 160-turn 16-layer PCB coil

or

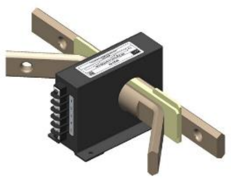

DCCT

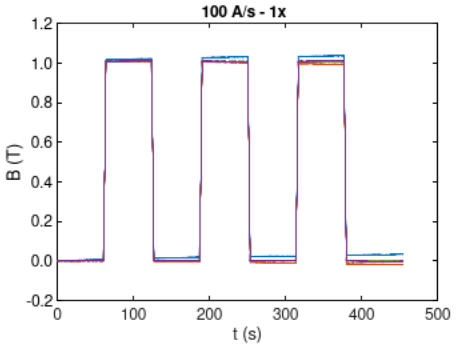

Stable (repeated) cycles

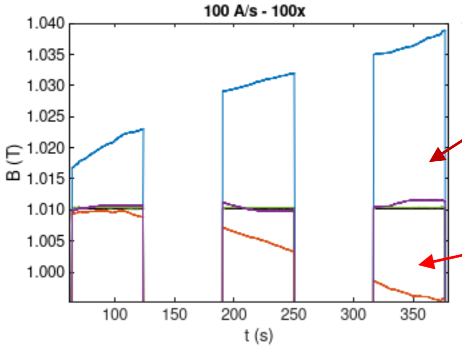

Uncorrected drift 60 ppm/s

V_0 updated on each plateau 3 ppm/s

V_0 estimated on first plateau 53 ppm/s

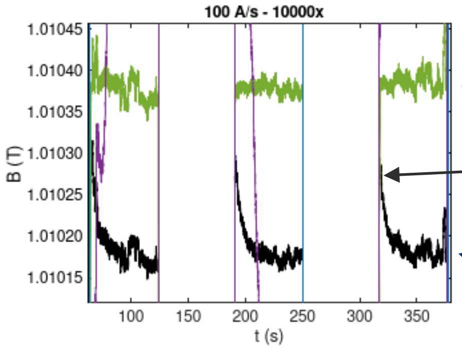

Kalman + exc. current 0.08 ppm/s

Actual eddy current decay transient

Kalman + Hall probe 0.03 ppm/s

V. Di Capua, M. Pentella *et al.*, *"Drift-free integration in magnetic measurements achieved by data fusion ", Sensors 2022, 22, 18*

Machine Learning: hysteresis modelling

- Very promising approach for the interpolation of non-linear dynamical effects (hysteresis, eddy currents)
- In progress: real-time implementation for bending field control

Modelling the pole field of a small test quadrupole
On the right, a sequence of training cycles with gradually increasing flat-top.

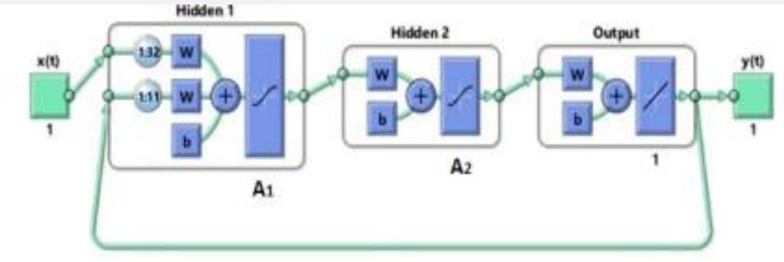

3-layer, 8-node autoregressive NN implemented in Matlab.

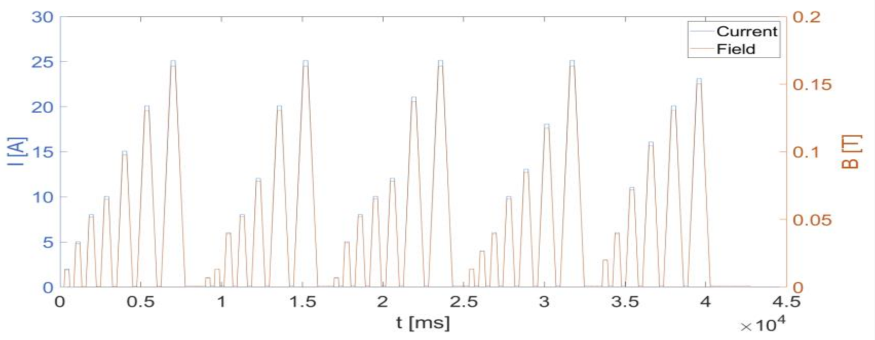

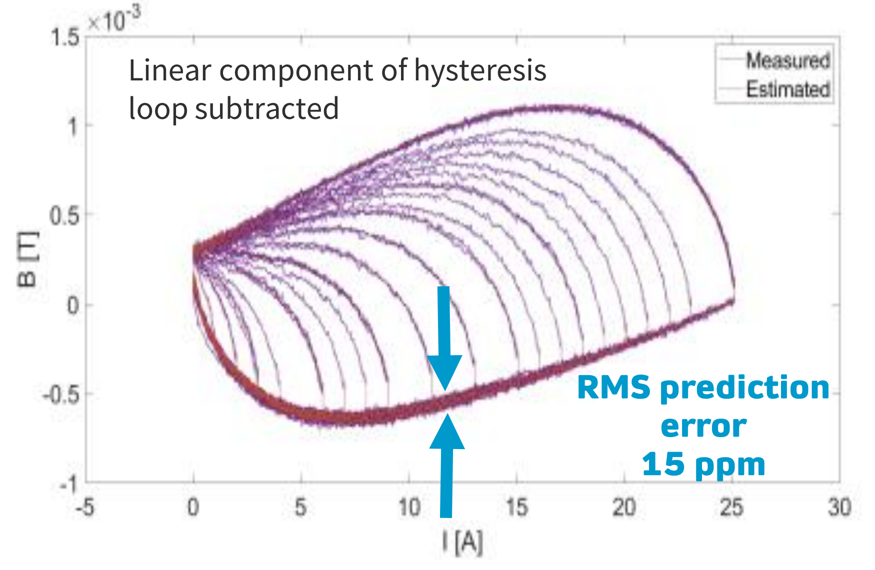

Comparison prediction/measurement on cycles with increasing, but different flat-top levels respect to training (only the non-linear component is shown in the figure). In this simple case, the interpolating capability of the autoregressive NN is excellent.

(V Di Capua, "Hysteresis modeling in iron-dominated magnets based on a Deep Neural Network approach", *Int. Journal of Neural Systems*)

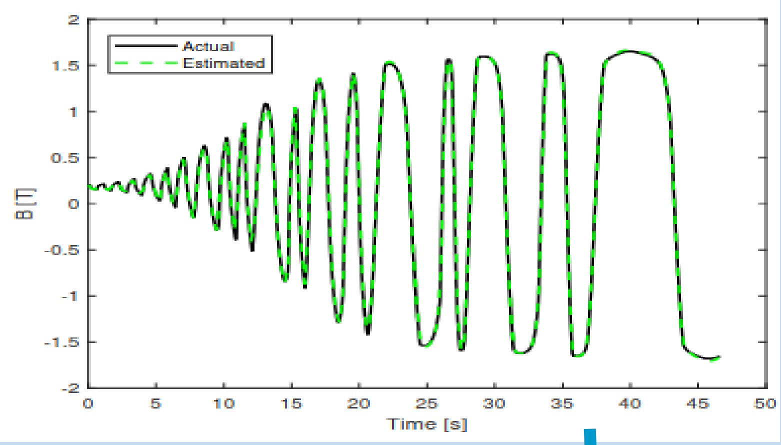

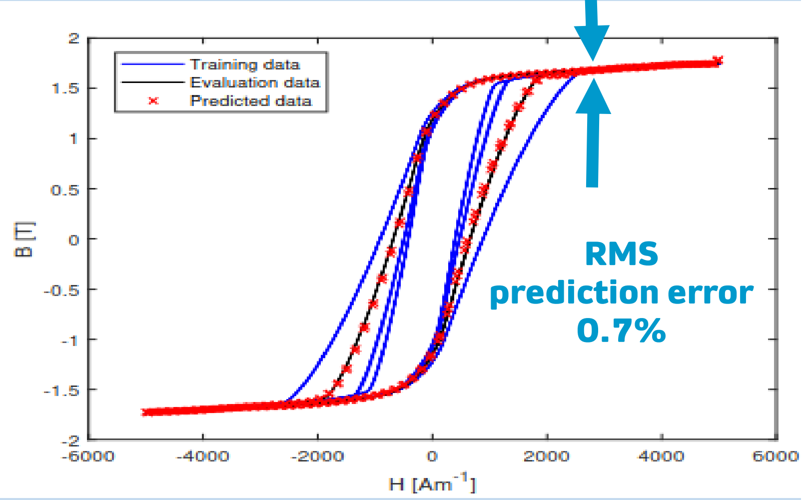

ARMCO ring sample with varying excitation ramp rate

(M Pentella, "Dynamic Ferromagnetic Hysteresis Modelling using a Preisach-Recurrent Neural Network Model", MDPI materials)

Conclusions

Conclusions

- Magnetic measurements are crucial to qualify accelerator components, complementing calculations and beam measurements. Scarce offer of commercial products → **in-house development is a strategic long-term priority**
- CERN offers **unique world-class test infrastructure** and capabilities, regularly updated to keep up with the evolution of requirements and technology.
- Current R&D axes: **off-the-shelf**/industrially available/cost-driven components; **calibration** techniques and uncertainty analysis; **combining pling EM physics**/computational models to measurement procedures
- Very busy with HL-LHC…. but we value open exchange and discussion and **look forward to collaboration proposals** with scientific partners

Upcoming Events

CERN Accelerator School On Magnets

19.11 – 02.12.2023 St. Pölten, Austria

	19/11	20/11/23	21/11/23	22/11/23	23/11/23	24/11/23	25/11/23	26/11/23	27/11/23	28/11/23	29/11/23			2/12
	Sun	Mon	Tue	Wed	Thu	Fri	Sat	Sun	Mon	Tue	Wed	Thu	Fri	Sat
08:30	Arrival day and registration	Opening F.Tecker local speakers	Field description for magnets	Magnetic field computation using FEM	Technical superconductors (LTS)	Quench detection & magnet protection	Powering infrastructures	Excursion	Superferric magnets	Material for magnets & measurements I		Metrology, alignment & fiducialisation	Dielectric insulation & HV issues	Departure day
09:30		Vector Algebra and Analysis	Basics of numerical field computation	RT magnet design, fabrication, testing III	SC magnet design - EM part II	Hands-on block 2	Magnetic measurement systems overview		SC dynamic field effects	Heat transfer, cryostat, conduction cooling II		SC magnet fabrication + testing I	Permanent magnets	
10:30		Coffee							Coffee			Coffee		
11:00		Basics on electrotechniques & Maxwell Equations I	Introduction to practical exercises - Superconductivity	SC magnet design - EM part I	Technical superconductors (HTS)	Hands-on block 2	Rotating coils, flux metric method, wire systems		Heat transfer, cryostat, conduction cooling I	Material for magnets & measurements II		Injection & extraction devices	Low-emittance ring magnets	
12:00		Basics on electrotechniques & Maxwell Equations II	Introduction to practical exercises - Magnetic Measurements	SC magnet design - mechanical I	SC magnet design - mechanical II		Mapping techniques (Hall Probes)		NC dynamic effects, reproducibility	NC Modelling & measurement of non-linear effects		SC magnet fabrication + testing II	Magnets for medical applications	
13:00		Lunch							Lunch					
14:30		Beam dynamics + resulting magnet specifications II	RT magnet design, fabrication, testing I	Hands-on block 1		Medaustron Visit	Hands-on block 2		Hands-on block 3		Hands-on block 4		Insertion devices	
15:30		Beam dynamics + resulting magnet specifications I	Superconductivity										Collider magnets (incl. muon collider)	
16:30		Coffee					Coffee		Coffee					
17:00		One slide - one minute All	RT magnet design, fabrication, testing II	Hands-on block 1			Hands-on block 2		Hands-on block 3		Hands-on block 4		Closing F.Tecker	
18:00		Welcome Drink			Poster Session									
19:30	Dinner												Special Dinner	
21:00										Social Event				v1.00

International Magnetic Measurement Worskop IMMW 23

07 – 11.10.2024, PSI, Villigen